Technical Reference for
ET2001 Thermal Voltage Converters

(Version 3.01, 15/Apr./2010)

Nano-Electronics Research Institute / AIST, Japan

About This Manual

This manual, "Technical Reference for ET2001 Thermal Converters", provides technical information about the special TVCs used in the ET2001 AC-DC Standard system (hereafter referred to as “ADS” system).

Contents of the other manuals are as follows:

“Quick-Start Manual for ET2001 ADS system”
This manual provides technical information for the use of ET2001 ADS system, including comprehensive guidance for installation and initial setting-up of the equipment.

"A Guide for establishing primary AC-DC transfer standard using ET2001 ADS system"
This manual provides detailed technical information about the operation of ET2001 ADS, and its application for the evaluation of thermal converters to establish a primary AC-DC transfer standard.

"Technical Reference for ET2001 ADS system Hardware"
This manual provides detailed technical information about hardware of the ET2001 ADS system, including the interfacing commands and circuit descriptions.

The organization of the manual is to first provide a simple overview of AC-DC transfer standard using a thermal converter in chapter 1. Subsequent chapters (Ch.2 - Ch.4) provides detailed description of the three type of TVCs, i.e., TVC04, TVC05 and TVC06, followed by summary of specification (Chapter 5) and supplementary information (Chapter 6).

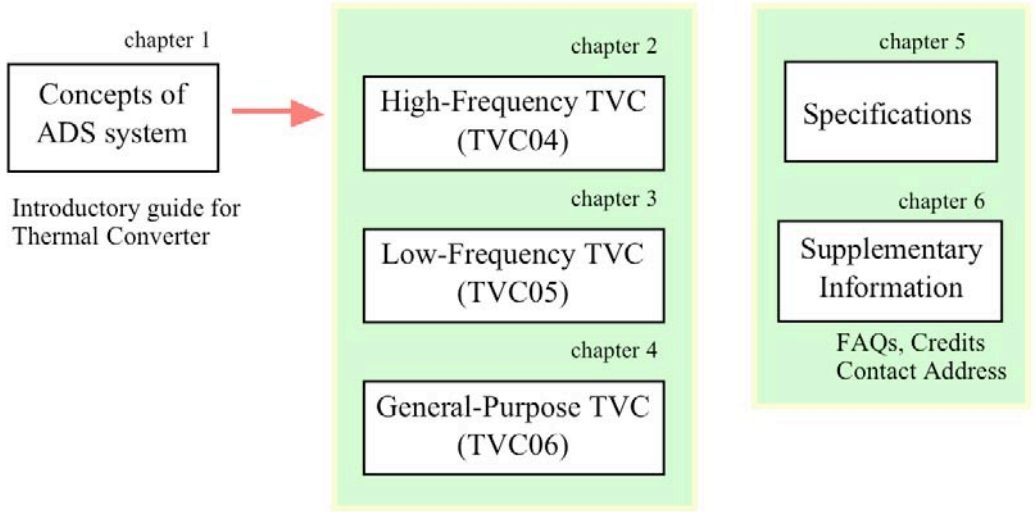

Important Notes

CAUTION! **--- Overloading of the TVC by more than 200% of the nominal input power may cause permanent damage to the TC element.**

CAUTION! **--- Electrostatic discharge to the output of the TVC may result in the static breakdown in the thermopile output.**

NOTE **--- TVC05 is optimized for operation at frequency <100 Hz, and has relatively large time constant (normally 6 s).**

NOTE **--- TVC04 is optimized for operation at >10 kHz, and may have a low-frequency error up to a few ppm at <100 Hz).**

Table of Contents

1. Introduction 6
1.1. Background 6
1.2. AC-DC Transfer Standard 6
1.2.1. AC-DC Difference 6
1.2.2. Thermal Converter 7
1.3. Determination of Frequency Characteristics 9
1.3.1. DC Characteristics 9
1.3.2. Low-Frequency Characteristics 10
1.3.3. High-Frequency Characteristics 11
1.4. Principles of Measurements 11
1.4.1. FRDC-DC Difference Measurement 11
1.4.2. ACLF-AC Difference Measurement 14
1.4.3. AC-DC Difference Measurement 15
2. High-Frequency TVC (TVC04) 17
2.1. Type-JSTC04 TC Element 17
2.2. Built-in TEE configuration 18
2.3. Mathematical Model 19
2.4. Measurement of Parasitic Components 21
2.4.1. Lead Inductance and Skin Effect 21
2.4.2. Stray Capacitance of Heater 22
2.4.3. Capacitance Between Heater and Thermopile 23
2.5. Evaluation of Frequency Characteristic 24
2.6. Uncertainty due to Built-in TEE 26
3. Low-Frequency TVC (TVC05) 28
3.1. Type-JSTC05 TC Element 28
3.2. Evaluation of Frequency Characteristics 29
3.2.1. AC-LF measurement 29
3.2.2. Impedance-matching method 30
3.2.3. 90-degrees-addition method 32
4. General-Purpose TVC (TVC06) 36
4.1. Type-JSTC06 TC Element 36
4.2. Evaluation of Frequency Characteristics 37
4.2.1. DC Characteristics 37
4.2.2. Low Frequency Characteristics 38
4.2.3. High Frequency Characteristics 38
4.2.4. Over-all Characteristic 39
Specifications 41
4.3. TVC04 41
4.4. TVC05 41

4.5. TVC06 42

5. Supplementary Information 44

5.1. FACs 44

5.2. Acknowledgements 44

5.3. Contact Address 44

1. Introduction

1.1. Background

DC voltage standards precise to 10^{-9} are achievable with Josephson junction devices. High precision for AC voltages, even to 10^{-7} are much more difficult to measure, so that the method to set an AC standard most commonly used is through the "transfer" or comparison with a precision DC standard. This is achieved by comparing the RMS power of the AC voltage with that of the standard DC using a thermal converter. AC voltage standards in the frequency range between 10 Hz and 1 MHz can thus be derived. However, because every electrical system is subject to noises from many sources, with many dependent on the frequency, predetermined corrections must be added to the measurements to compensate for these and to calibrate the equipment under test. Especially troublesome are non-negligible heating or cooling during the DC input mode. These Thomson and Peltier thermoelectric effects give rise to frequency-independent AC-DC differences at a 10^{-6} level [1]. Because of the difficulties in avoiding or evaluating the thermoelectric effects in a thermal converter, only a limited number of national metrology institutes have been able to establish independent primary standards of AC-DC transfer. Since 2001, the AIST in Japan [3] uses the Fast-Reversed DC (FRDC) method to evaluate the frequency independent AC-DC difference in the transfer standard.

FRDC was developed in the 1990's, aiming at the experimental determination of the thermoelectric effects in thermal converters [2]. The FRDC method is based on the assumption that, if the frequency of the polarity reversal in a rectangular FRDC waveform is much faster than the thermoelectric time constant, the thermoelectric effects do not affect the temperature distribution.
This document describes a second-generation FRDC instrument, ET2001 AC-DC Standard (ADS) System, developed at AIST in cooperation with Sunjem Co. Ltd, Japan. The new instrument includes not only the FRDC source, but also a complete miniature AC-DC comparator system, consisting of a DSS module, TC/AMP modules, and Thermal Converters. The system may be used to establish an independent primary AC-DC transfer standard in calibration laboratories.

1.2. AC-DC Transfer Standard

1.2.1. AC-DC Difference

The ac voltage is defined by the root-mean square (rms) value of the sinusoidal waveform:

$$V_{AC}(rms) \equiv \sqrt{\frac{1}{T}\int_0^T \{V(t)\}^2 dt} \qquad (1.1)$$

In accordance with this definition, it is possible to compare an ac voltage with a dc voltage by alternately applying them to the same heater in a thermal converter (TC) and measuring the temperature rise with a thermocouple. When dc and ac voltages that result in equal power output are applied to the input of an ideal thermal converter, the resultant EMFs are the same. In the case of an actual TC, however, the output EMFs are influenced by the effect of non-joule heating and the frequency dependent characteristics of the heater circuit. The AC-DC transfer difference is conveniently defined by the following equation.

$$\delta_{AC-DC} \equiv \left. \frac{V_{AC} - V_{DC}}{V_{DC}} \right|_{E_{AC}=E_{DC}} \tag{1.2}$$

The quantities E_{DC} and E_{AC} represent the output EMFs of the thermocouple when the dc voltage V_{DC} and the ac voltage V_{AC}, respectively, are applied to a thermal converter.

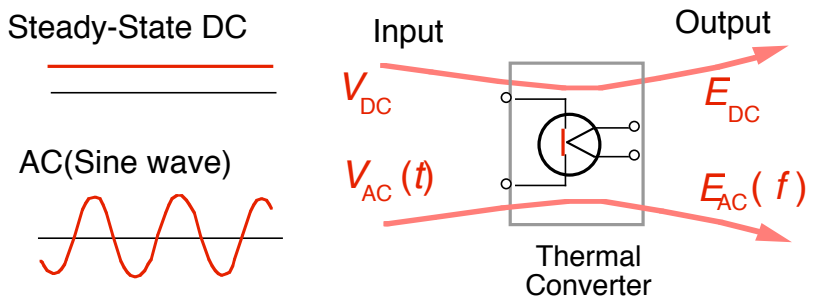

Fig. 1.1 Thermal converter for AC-DC transfer Standard

1.2.2. Thermal Converter

The most accurate AC-DC transfer standards are realized by the use of "thermal converters". Single-Junction Thermal Converters (SJTCs) were developed in the 1950s. The structure of a typical SJTC element is shown in Fig. 1.2. A thin filament-heater and a thermocouple are enclosed in an evacuated glass bulb. The thermocouple junction is in thermal contact with the heater at the midpoint of the heater, but is electrically insulated from it by a bead of glass or ceramic.
Multijunction Thermal Converters (MJTCs) were developed in the 1970s-1980s. The MJTCs are designed to suppress the Thomson and Peltier effects. These are the main cause of the AC-DC transfer difference around 1 kHz. The structure of type-JSTC04 thermal converter element, developed at AIST in cooperation with Nikkohm Co., is illustrated in Fig. 1.3. The thermopile (thermocouples connected in series) is formed on a thin polyimide membrane supported by an alumina (Al2O3) frame. The heater is formed on an AlN (aluminum nitride) chip mounted on the polyimide membrane. The thermal converters are capable of comparing the joule heating between ac and dc modes at 0.1 ppm level, and are widely employed as the primary standard in most national standard laboratories.

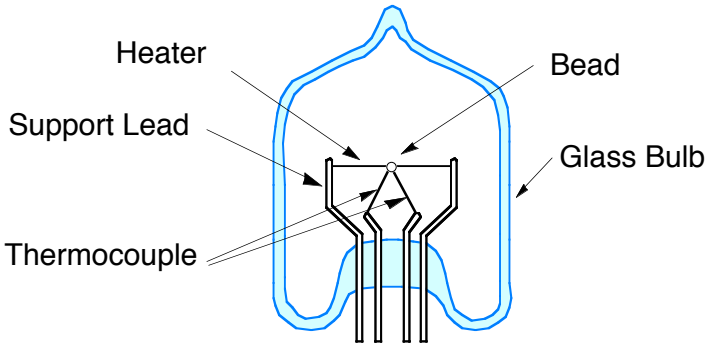

Fig. 1.2 Structure of Single-Junction Thermal Converter

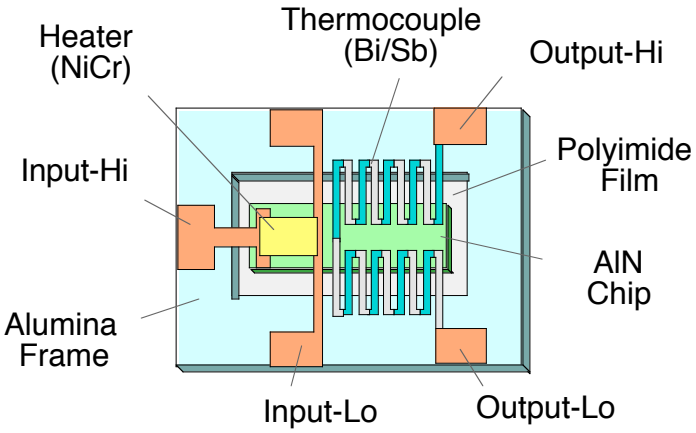

Fig. 1.3 Structure of JSTC04 Multi-Junction Thermal Converter

There are three main causes of the AC-DC transfer difference:

(1) Thermoelectric effect (dc offset): When the dc current is passed through the heater of a thermal converter, non-joule heating/cooling takes place along the heater due to thermoelectric effects such as the Thomson or Peltier effect. In the case of SJTC with standard construction, an AC-DC difference of a few ppm is observed due to the thermoelectric effects.

(2) High-frequency characteristic: In the frequency range above 10 kHz, the skin effect of the conductor and the stray inductance and capacitance in the input circuit become significant. When a standard-design SJTC-element is combined with a current-limiting metal-film resistor of 1kΩ, the effect to the AC-DC transfer difference is of the order of 0.1 ppm, 1 ppm, and 100 ppm at the frequency of 10 kHz, 100 kHz, and 1 MHz, respectively.

(3) Low-frequency characteristics: The thermal time constant of a standard-design SJTC-element is about 1 s. At frequencies below 100 Hz, double-frequency thermal ripple is created due to insufficient thermal inertia. In the case of a standard SJTC, the effect to the AC-DC difference is of the order of 0.1 ppm and 10 ppm at 100 Hz and 10 Hz, respectively.

The AC-DC transfer difference of a thermal converter over the 100 Hz to 1 MHzfrequency range is given in equation 1.3. The three components are as follows:

LF: low frequency component
HF: high frequency component
TE: thermoelectric effects

$$\delta_{AC-DC} \cong \delta_{LF}(f) + \delta_{HF}(f) + \delta_{TE} \qquad (1.3)$$

The typical frequency characteristic of a thermal converter is illustrated in the figure. Frequency characteristic of a thermal converter can be evaluated using special thermal converters (TVC04 and TVC05), as described in subsections 1.3.2 and 1.3.3. The thermoelectric effects, which occur at the dc-mode, give the frequency-independent offset in the AC-DC difference. Since both the low-frequency characteristic and the high-frequency characteristic reduce below 0.1 ppm in the frequency range between 100 Hz and 10 kHz, the AC-DC difference in this range is predominately a DC offset due to the thermal effects and is not frequency dependent.

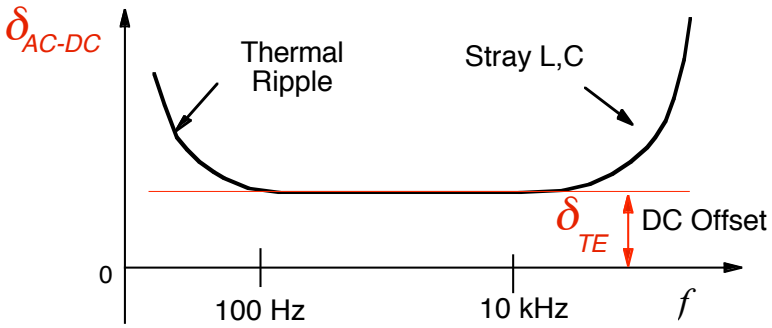

Fig. 1.4 Frequency characteristic of a thermal converter

1.3. Determination of Frequency Characteristics

1.3.1. DC Characteristics

The major source of the frequency-independent AC-DC difference is the second-order Thomson effect. The typical temperature distribution along the heater due to Joule-heating is shown in Fig. 1.5(a). When the Thomson effect is present, the electric current influences the heat flow and modifies the temperature gradient along the heater. The change in temperature distribution due to the Thomson effect is shown in Fig. 1.5(b). The Thomson effect can result in a temperature distribution as large as 0.1 K. However, most of the effects are canceled to the first-order by reversing the polarity of the current and taking the mean. The temperature gradient due to the second-order Thomson effect is of the order of a few mK, as shown in Fig. 1.5(c), and contributes

to the AC-DC difference at the ppm level. The AC-DC difference due to the second-order Thomson effect can be evaluated using the formula by Widdis:

$$\delta_{ac-dc} = -\frac{1}{12}\frac{\sigma^2\theta_0}{\rho k} \qquad (1.4)$$

The symbols σ, θ_0, ρ, and κ represent the Thomson coefficients, mid-point temperature-rise, electric resistivity, and the thermal conductivity of the heater. In the case of standard SJTCs, the thermal transfer difference is of the order of a few parts in 10^{-6}. The thermoelectric effects in thermal converters can be evaluated by the "fast-reversed dc" method.

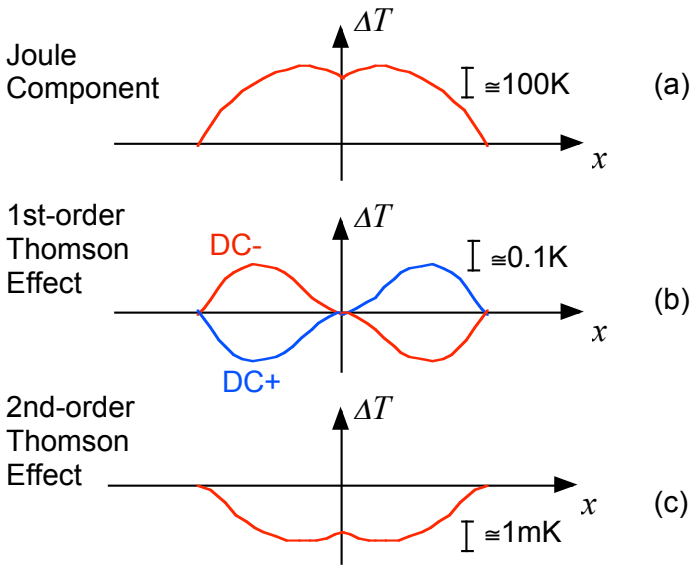

Fig. 1.5 Temperature distribution along heater

1.3.2. Low-Frequency Characteristics

When sinusoidal voltage of frequency *f* is applied to a TVC (thermal voltage converter), joule heating varies with double-frequency, 2*f*. If the frequency is sufficiently high, i.e., if the thermal time constant τ is much longer than the period of the double-frequency heating ($\tau >> 1/f$), the variation of temperature becomes negligible due to the thermal inertia of the heater. At frequencies below 100 Hz, thermal inertia of the heater becomes insufficient to suppress the double-frequency thermal ripple. The thermal ripple causes the AC-DC difference of a TVC due to the imperfections in the SJTC elements:

(a) Non-linearity of input-output characteristic of TVC.
(b) Frequency dependence of the heater-resistance.
(c) Imperfect averaging of the voltage ripple in EMF output.

In the case (c), the effect to the AC-DC difference may be reduced by use of a low-pass filter or by setting the integration time of a DVM to the multiple of the input frequency. While in cases (a) and (b), the effects are based on the thermal properties of the SJTC elements, and the contribution to the AC-DC difference has to be evaluated.
The low-frequency performance of a thermal converter may be evaluated by two methods using the ET2001 ADS system, i.e., (1) Impedance-matching method and (2) AC-LF measurement (synthesized-waveform method).
In the case of the Impedance-matching method, AC-DC difference of a TVC is compared against another TVC of the same type using a special comparison circuit, such that one of the TVC is operated at much smaller power level than the other. In the case of the AC-LF measurement, a synthesized waveform source (DSS module) is used as a reference standard, and the change in the output EMF from the TVC is measured by a DVM (AMP module). This method is described in detail in section 1.4.2.

1.3.3. High-Frequency Characteristics

Operating at above 10 kHz, the frequency characteristic of the TVC-input circuit due to the skin effect, dielectric loss, and the stray inductance and capacitance becomes non-negligible compared with thermoelectric effects. Beyond 100 kHz, the frequency characteristic contributes more than 1 ppm and becomes the dominant term in the AC-DC transfer difference.
Since the impedance of the input circuit determines the frequency characteristic of a TVC, it is quite important do define the reference plane of the input circuit from which the AC-DC difference is defined. Usually, the reference plane is taken at the center of a TEE connector directly connected to the input of a TC or TC module. The primary standard in the high-frequency characteristic of AC-DC difference is realized by a specially designed TVC (TVC04), which has a special construction so that its high-frequency characteristic is calculable from its structure and dimensions. The design and the performance of the TVC04 is described in detail in chapter 2.

1.4. Principles of Measurements

1.4.1. FRDC-DC Difference Measurement

Until the late 1990's, the ac-dc transfer standard in Japan had an uncertainty of 10 ppm. This precision was not good enough to calibrate new instrumentation. Application of the "Fast-Reversed DC" (FRDC) method, developed at PTB (Physikalisch-Technische Bundesanstalt), has allowed ten-fold improvement in the uncertainty of the national standard. The purpose of the method is to evaluate the thermoelectric transfer difference experimentally, as illustrated in Fig. 1.6. For simplicity, only the Thomson effect along the heater is shown in the figure. When dc current passes through a thermal converter, the temperature distribution is modified due to the Thomson effect as shown in Fig. 1.6(a). When the current is reversed, the polarity of the Thomson effect is also reversed, resulting in a different temperature distribution along heater as shown in Fig. 1.6(b). The characteristic time constants of the change in the temperature distribution due to the Thomson and

Peltier effects are determined by the structure and material of the heater, hereafter called "thermoelectric time constants". In the case of FRDC mode, if the reversal of the current is slow enough compared with the thermoelectric time constants, the same temperature distribution along the heater is obtained as that for the steady-state dc, as shown in Fig. 1.6(c). Hence the average output EMF of thermal converter in the slow-reversing mode is equal to the mean output EMF for DC+ and DC- modes, and the FRDC-DC difference becomes zero. On the other hand, if the reversal of the current is fast enough, thermoelectric effects do not have enough time to develop during one current direction, and the influence of thermoelectric effects is reduced to zero, as shown in Fig. 1.6(d). In this case, the FRDC-DC difference equals to the thermoelectric effect in dc modes.

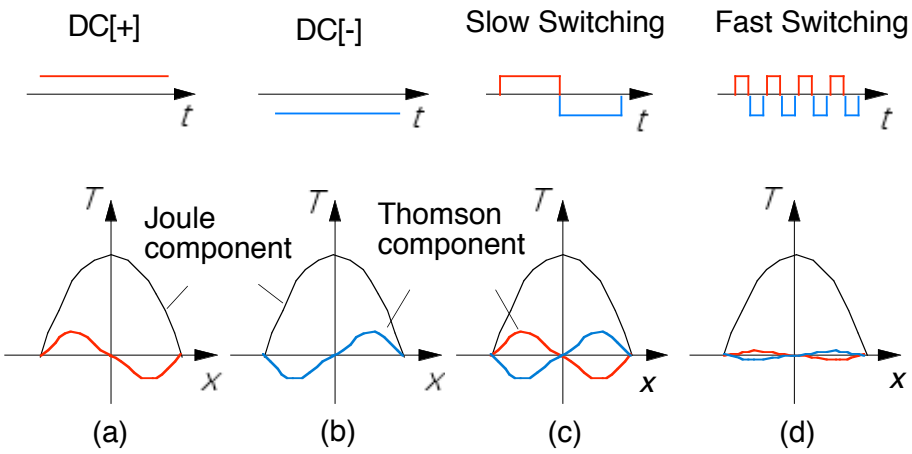

Fig. 1.6 Thermoelectric effects in thermal converters with the FRDC waveform.

In the FRDC-DC difference measurement, rectangular-waveform are synthesized by switching between a positive dc source (DC+) and a negative dc source (DC-) as illustrated in Fig. 1.7. The switching is performed using high-speed analog switches. If the switching is performed in a perfect way, a high-precision rectangular ac waveform is obtained whose rms power is equal to the mean of the two dc sources. The rectangular waveform synthesized in this way is called the Fast-Reversed DC (FRDC) waveform, and the circuit for producing the FRDC waveform is called the FRDC source. Following the definition of the AC-DC difference of a thermal converter given by (1.2), an "FRDC-DC difference" $\delta_{FRDC\text{-}DC}$ is defined as follows:

$$\delta_{FRDC-DC} \equiv \left. \frac{V_{FRDC} - V_{DC}}{V_{DC}} \right|_{E_{FRDC}=E_{DC}} \qquad (1.5)$$

Here, E_{FRDC} represents the EMF for the FRDC waveform, and E_{DC} represents the mean EMF for the DC+ and DC- waveform. A modified waveform shown in Fig. 1.8 is used in the actual FRDC sources. Since the same number of positive edges and negative edges are included in DC and FRDC waveform, the effect from switching transients and high frequency components are canceled between the DC and FRDC modes.

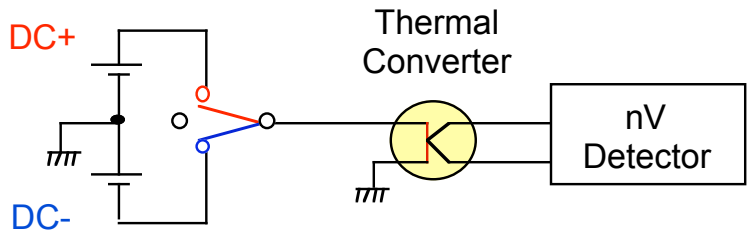

Fig. 1.7. FRDC-DC difference measurement circuit.

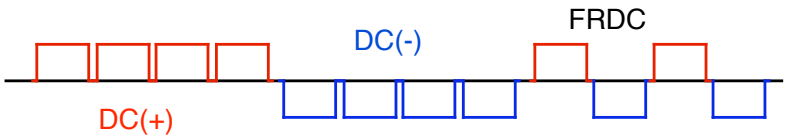

Fig. 1.8 Modified DC and FRDC waveforms.

In this method, the Nono-Voltmeter measures the output EMF voltages from the TVC. If the difference between the voltages V_{FRDC} and V_{DC} is small, the input-output characteristic can be approximated to be linear in the low voltage range. In this case, the following approximation is possible:

$$V_{FRDC} \cong V_{DC} + \left[E_{FRDC} - E_{DC}\right]/k$$

$$\text{Where, } k = \frac{\Delta E}{\Delta V}. \qquad (1.6)$$

Here, ΔE represents the change in the EMF output from the TVC when a small change in the input voltage ΔV is applied. Substituting (1.6) to (1.5), the FRDC-DC difference $\delta_{FRDC\text{-}DC}$ is determined by the following equation:

$$\delta_{FRDC-DC} \cong -\frac{E_{FRDC} - E_{DC}}{nE_{DC}}$$

$$\text{Where, } n = \frac{(\Delta E / E)}{(\Delta V / V)} \qquad (1.7)$$

The 'normalized index n is of the order of 2 for the TVCs with square-output characteristics. In the case of modified waveform, the quantities E_{FRDC} and E_{DC} represent the average EMFs for the two MDFR modes and for the two CPDC modes respectively, as defined by,

$$E_{FRDC} \equiv \frac{E_{MDFR(1)} + E_{MDFR(2)}}{2}, \quad E_{DC} \equiv \frac{E_{CPDC+} + E_{CPDC-}}{2} \qquad (1.8)$$

1.4.2. ACLF-AC Difference Measurement

As discussed in section 1.3.2, the low-frequency performance of a thermal converter may be evaluated by two methods using the ET2001 ADS system, i.e., (1) Impedance-matching method and (2) the AC-LF measurement (synthesized-waveform method) which is described in this section. In this measurement, a synthesized waveform source (DSS module) is used as a reference standard. The change in the output EMF from the TVC is measured by a DVM (AMP module).
The "ACLF-AC difference" δ_{ACLF} is defined using the following definition.

$$\delta_{ACLF} \equiv \left. \frac{V(f) - V(f_0)}{V(f_0)} \right|_{E(f)=E(f_0)} \tag{1.9}$$

Here, $E(f)$ represents the EMF at the test frequency f, and $E(f_0)$ represents the EMF at the reference frequency f_0.
The schematic diagram of the measurement circuit is shown in figure 1.9. In this method, the main detector is the DVM (ADC in TC module) which measure the output EMF voltages from the TC element.

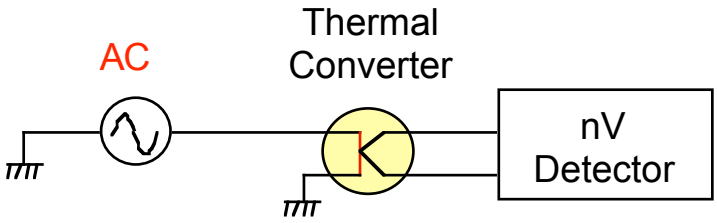

Fig. 1.9 AC-LF Measurement Circuit.

As in the case of the FRDC-DC difference measurement, if the difference between the voltages $V(f)$ and $V(f_0)$ is small, the input-output characteristic can be approximated to be linear in the small voltage range. In this case, the following approximation is possible:

$$V_{AC}(f) \cong V_{AC}(f_0) + \left[E(f) - E(f_0)\right]/k$$

$$\text{Where} \quad k = \frac{\Delta E}{\Delta V}. \tag{1.10}$$

Substituting (1.10) to (1.9), the ACLF difference δ_{ACLF} is determined by the following equation:

$$\delta_{ACLF} \cong -\frac{E(f) - E(f_0)}{nE(f_0)}$$

$$\text{Where,} \quad n = \frac{(\Delta E / E)}{(\Delta V / V)} \tag{1.11}$$

Normalized index "*n*" is of the order of 2 for the TVCs with square-output characteristics.

1.4.3. AC-DC Difference Measurement

The purpose of the AC-DC difference (comparison) measurement is to determine the relative difference in the AC-DC difference between two TVCs, usually specified as TC(X) and TC(S). The ET2001 ADS system performs the AC-DC difference measurement based on the dual-channel method. The schematic diagram of the dual channel method is shown in Fig. 1.10. In this method, the two nV-detectors measure the output EMF voltages of the two TVCs separately.

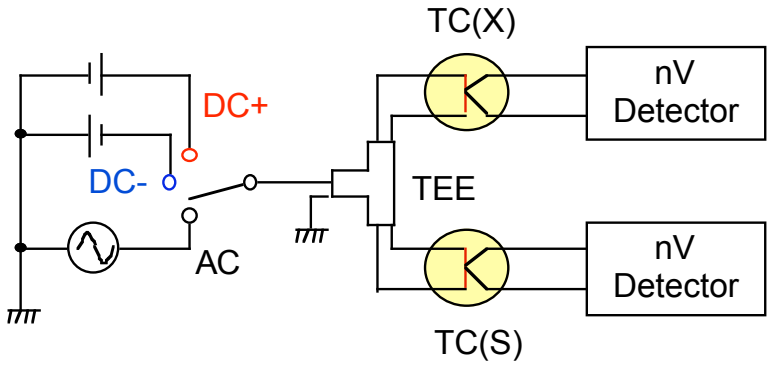

Fig. 1.10 AC-DC difference measurement circuit.

The input-output characteristics of the two TVCs are shown in Fig. 1.11. The EMF output of a TVC is approximately proportional to the square of the input voltage. The output-quantity X_{DC} and S_{DC} represent the EMF outputs from TVC(X) and TVC(S) for the dc input voltage V_{DC}. Similarly, the output-quantity X_{AC} and S_{AC} represent the EMF outputs for the ac input voltage V_{AC}. The input-quantity V_X and V_S represent the ac input voltages which produce the same EMF voltage (X_{DC}, S_{DC}) as in the case of applying the dc input voltage V_{DC}.
Using the definition of the AC-DC difference of a TVC given in (1.2), the relative AC-DC difference between TVC(X) and TVC(S) is deduced as

$$\delta_X - \delta_S \equiv \left.\frac{V_X - V_S}{V_{DC}}\right|_{\substack{X_{AC}=X_{DC} \\ S_{AC}=S_{DC}}} . \qquad (1.12)$$

If the difference between the dc input voltage V_{DC} and ac input voltage V_{AC} is small, the input-output characteristic of the two TVCs may be approximated to be linear in the small voltage range. In this case, the following approximation is possible:

$$\begin{cases} V_X \cong V_{AC} + (X_{DC} - X_{AC})/k_X \\ V_S \cong V_{AC} + (S_{DC} - S_{AC})/k_S \end{cases}$$

$$\text{Where } k_X = \frac{\Delta X}{\Delta V},\ k_S = \frac{\Delta S}{\Delta V}. \qquad (1.13)$$

Here, ΔX and ΔS represent the change in the EMF output from TVC(X) and TVC(S) when a small change in the input voltage ΔV is applied. Substituting (1.13) to (1.12), the relative AC-DC difference $\delta_X - \delta_S$ is determined by the following equation:

$$\delta_X - \delta_S \cong \frac{S_{AC} - S_{DC}}{n_S S_{DC}} - \frac{X_{AC} - X_{DC}}{n_X X_{DC}}$$

$$\text{Where } n_X = \frac{(\Delta X / X_{DC})}{(\Delta V / V_{DC})},\ n_S = \frac{(\Delta S / S_{DC})}{(\Delta V / V_{DC})} \qquad (1.14)$$

The normalized indices n_X and n_S are of the order of 2 for the TVCs with square-output characteristics. Some of the semiconductor-based AC-DC transfer standards, like Fluke 792A or Datron 4920, have linear output characteristics, resulting in normalized indexes close to unity.

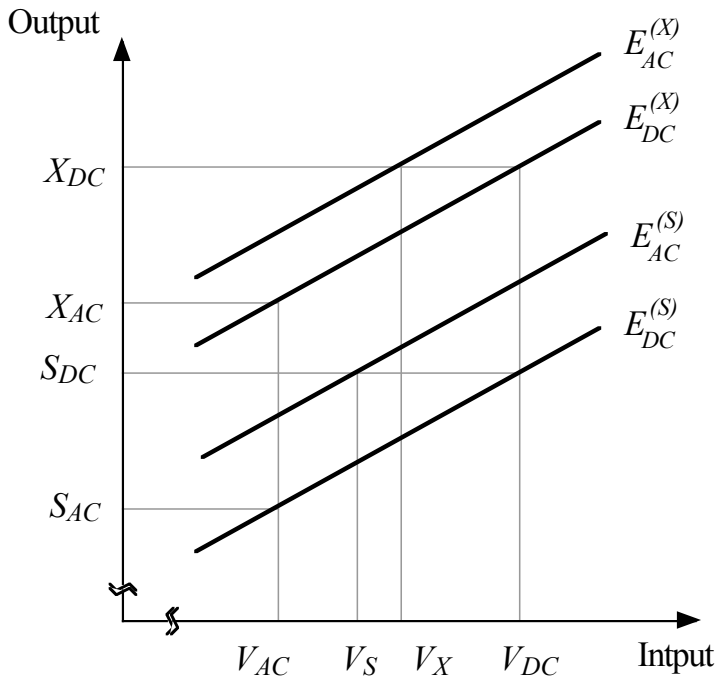

Fig. 1.11. Input-Output Characteristic

2. High-Frequency TVC (TVC04)

High-frequency characteristic of a TVC-input circuit becomes the dominant factor in the AC-DC transfer difference at frequencies higher than 100 kHz. In order to evaluate the high-frequency characteristics of TC modules up to 1 MHz, a High-Frequency-standard TVC (TVC04) has been developed at AIST, in collaboration with Nikkohm Co. Ltd. The TVC04 is designed such that the frequency characteristic is calculable from the shape and dimension of the input circuit. The thermal converter element (JSTC04) has a simple straight heater configuration, which reduces the parasitic impedence in the heater pattern. The internal-TEE (Virtual TEE) configuration has been used to avoid the effects from parasitic impedance in the input leads.

2.1. Type-JSTC04 TC Element

Various types of MJTCs have been developed by national standard laboratories to establish primary reference in AC-DC transfer standard. At the AIST, in cooperation with Nikkohm Co., a new thin-film MJTC have been developed as the core component of the ET2001 AC-DC transfer standard system. The new MJTC (Type JSTC04) is shown in Fig. 2.1.
As the thermoelectric effect can be evaluated experimentally by the FRDC method, emphasis in the design criteria was placed on the optimization of high-frequency characteristics, rather than reduction of thermoelectric effects. The layout of the new MJTC (Type JSTC04B) is illustrated in Fig. 2.2. The heater is sputtered onto a 2 mm x 8 mm AlN chip, mounted on a polyimide membrane with flip-chip bonding. The Bi/Sb thermocouples are formed on the polyimide membrane supported by an alumina frame as a heat sink. The basic design is the same as the commercial RMS-DC converter device (Nikkohm LP-35), except that the position of the thermocouples are separated from the heater, in order to reduce input-output coupling due to stray capacitance.
Input-Hi pattern has guard-electrode, which reduces the effect of stray capacitance between the heater and electrode, as described in the next section. Input-Lo pattern has two connecting terminals to realize co-planar return-path to the built-in TEE with minimum lead inductance. By the use of a thermopile consisting of 64 pairs of Bi/Sb thermocouple, sensitivity of 0.6 mV/mW is achieved. In the case of a nominal 5V MJTC element operating at 10 mA, an output EMF voltage of 30 mV is obtained. To increase the signal-to-noise ratio, the nominal output resistance of the MJTC is reduced to 400 Ω from a few kΩ used in the conventional design. Thermal response time is adjusted to about 3 sec by choosing a proper ratio for heat capacity of the AlN chip to thermal conductance across the thermocouples. Due to the good thermal conductivity of the AlN substrate, low-frequency dependence is suppressed to less than a few ppm down to 10 Hz.

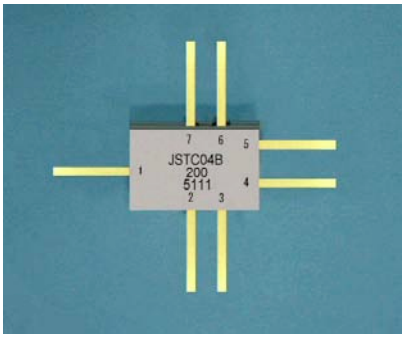

Fig. 2.1 JSTC04 Thermal Converter Element

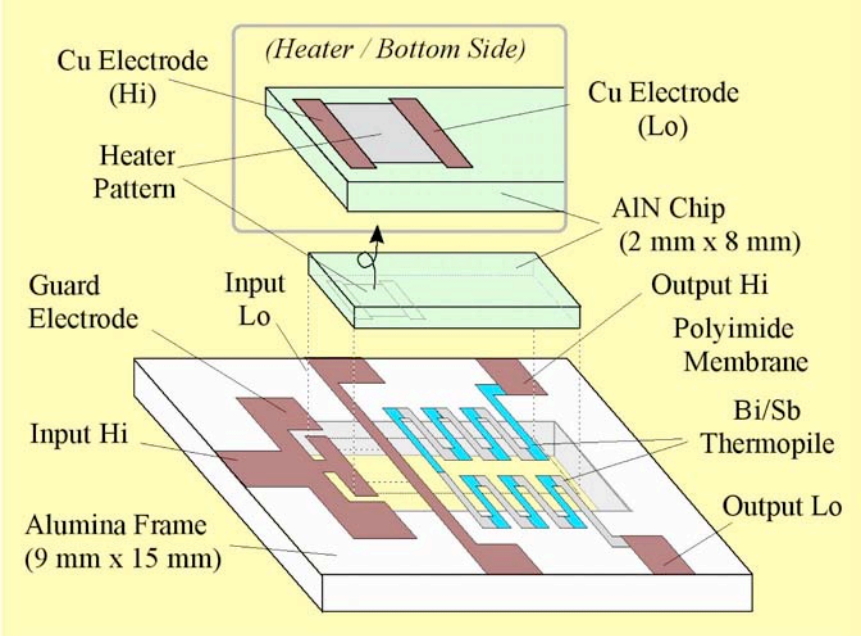

Fig. 2.2 Structure of JSTC04 Thermal Converter Element

2.2. Built-in TEE configuration

A picture and a cross-sectional view of a TVC04 are shown in Fig. 2.3 and Fig. 2.4, respectively. The AC-DC difference of a thermal converter is defined at the center-point of a TEE connector, and hence a built-in TEE configuration is used in order to take full advantage of the high frequency performance of the JSTC04 MJTC element. The MJTC element is mounted on a PCB, which connects both Hi and Lo input leads of the MJTC with shortest distance to the reference plane of built-in TEE.

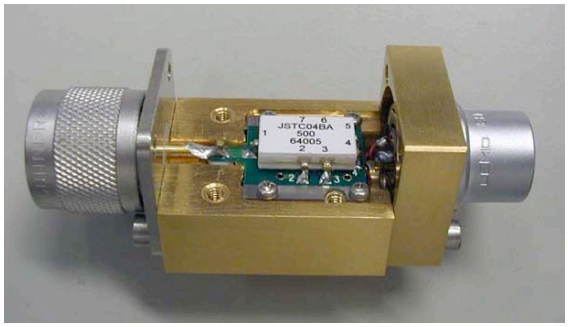

Fig. 2.3 Picture of a TVC04. The SMA connector is on the bottom side.

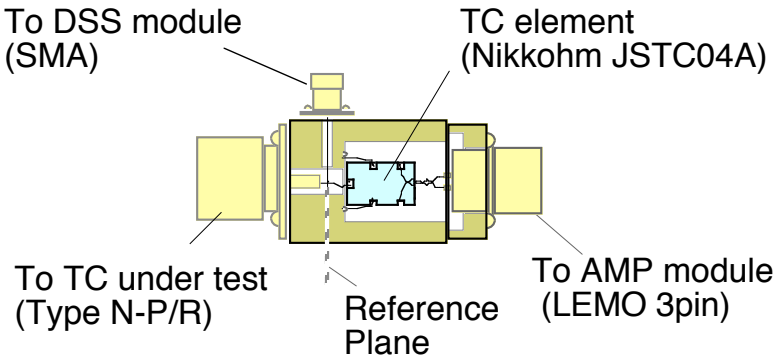

Fig. 2.4. Built-in TEE configuration of TVC04. TC element is rotated 90 degree from the actual position.

2.3. Mathematical Model

The frequency characteristic of the TVC04 is affected by parasitic components in the input circuit, such as lead inductance and stray capacitance, skin effect, and dielectric loss of the heater. The values of these parasitic components were evaluated using a mathematical modeling of the TVC04 [4]. The actual circuit configuration inside the TVC04, and corresponding circuit model with heater resistance r is shown in Fig. 2.5. A simplified input circuit model of the TVC04, taking asymmetric distribution of parasitic capacitance C_p into account, is shown in Fig. 2.6. L_p and R_{sk} are the parasitic inductance and skin effect of the leads from the built-in TEE to the heater. C_{p1}, C_{p2} and R_d represent the stray capacitances and dielectric loss between the two (Hi and Lo) electrodes of the heater.

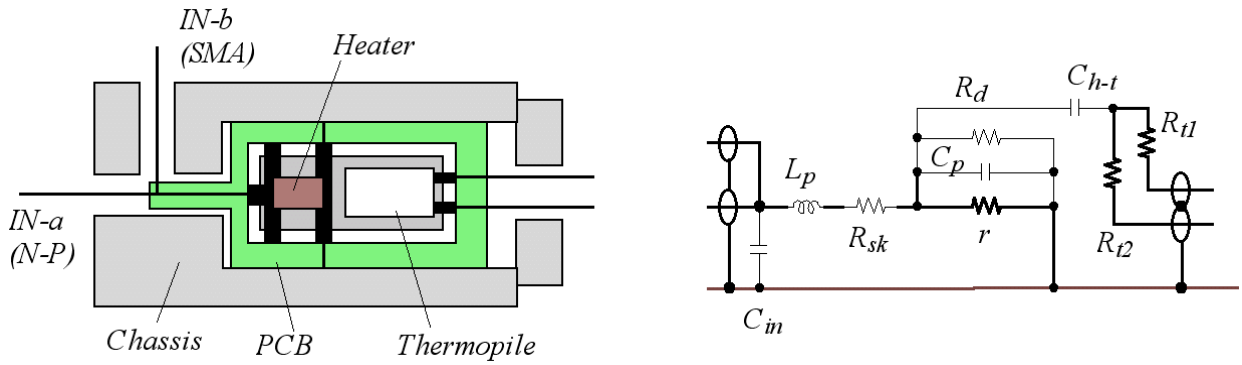

Fig. 2.5. Internal configuration and circuit model of TVC04.

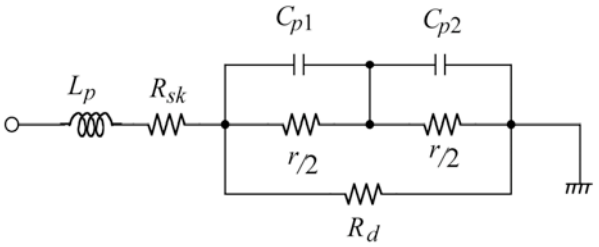

Fig. 2.6. Simplified model for input circuit of a TVC04.

Contribution of the five parasitic components to the AC-DC difference at high frequency range (10 kHz – 1 MHz) are calculated as:

$$\gamma \cong \gamma_{LR} + \gamma_{LC} + \gamma_{CR} + \gamma_{sk} + \gamma_{loss}$$

$$\begin{aligned}
\gamma_{LR} &= \frac{1}{2}\left(\omega L_p / r\right)^2 \\
\gamma_{LC} &= -\omega^2 L_p C_{p1} \\
\gamma_{CR} &= -\frac{1}{32}\omega^2 \left(\Delta C\right)^2 r^2 \\
\gamma_{sk} &= \frac{1}{2} R_{sk}(\omega) \Big/ r \\
\gamma_{loss} &= -\frac{1}{2} G(\omega) r
\end{aligned} \qquad (2.1)$$

$$1/C_p \equiv 1/C_{p1} + 1/C_{p2}$$
$$\Delta C \equiv C_{p1} - C_{p2}$$
$$G(\omega) \equiv 1/R_d$$

Here γ represents the frequency dependence of the AC-DC difference of a TVC04. The first two terms γ_{LR} and γ_{sk} represents the contribution from the parasitic inductance and skin effect of the lead. These are the dominant components for the low-resistance TVC. The terms γ_{CR} and γ_{loss} represents the effect of stray capacitance and dielectric loss of the heater that are dominant for the TVCs with higher heater resistance. Since the terms γ_{CR} goes to zero for a symmetric case (C_{p1}=C_{p2}), the parameter ΔC gives the measure of the contribution of the stray capacitances to the AC-DC difference. The last term γ_{LC} represents the LC resonance due to the parasitic inductance and the stray capacitance, which is independent of the resistance value.

Another source of uncertainty arises from the use of an N-P plug, to which a test-TVC is connected. As discussed in the previous section, the N-P plug imitates the half part of the N- RRR TEE connector by which the reference plane is defined. Hence, the difference in the shape and dimension of the N-P plug and the N- RRR TEE connector must be taken as a source of uncertainty in the calibration using the TVC04. In the case of an TVC04 with built-in TEE, the uncertainty due to the use of N-P connector dominates the over-all uncertainties below 100 kHz. The uncertainty may be evaluated experimentally, by adding an extra N-PR connector between TVC04 and test TVC.

2.4. Measurement of Parasitic Components

Some of the parasitic components (L_p, R_{sk}, C_p, R_d) of the TVC04 can be measured using an LCR meter in the frequency range of 10 kHz to 1 MHz. In addition to the four parasitic components of the input circuit, parasitic capacitance between the heater and the thermopile $C_{h\text{-}t}$ can be measured using the LCR meter. In the case of the TVC04, the thermopile pattern is guarded by the GND pattern of the heater, and it is shown that the contribution from the parasitic capacitance is reduced to a negligible level.

2.4.1. Lead Inductance and Skin Effect

To measure the inductance of the lead L_p and R_{sk}, the normal JSTC04 element should be replaced with a special "SHORT" element. In this element, the cupper film is deposited onto the heater pattern. The lead inductance and the skin effect may be measured by "L_s - R_s" configuration. The circuit connection inside the TVC04, and corresponding circuit model is shown in Fig. 2.7.

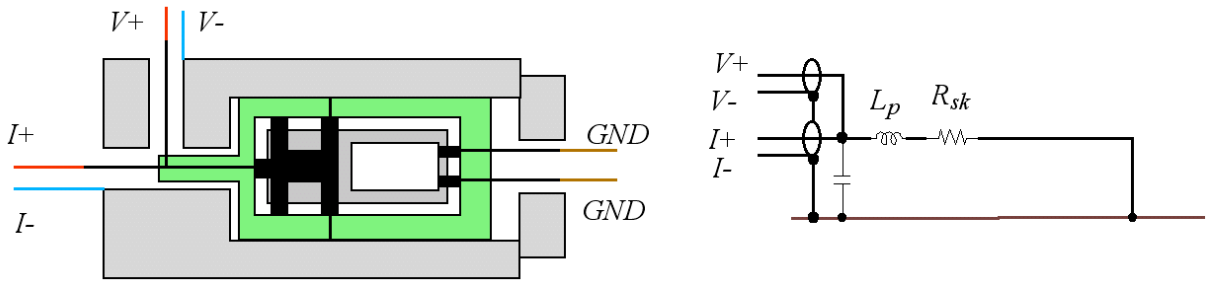

Fig. 2.7. Internal connection and circuit model for "L_s - R_s" measurement.

Typical results of the measurement are shown in Fig. 2.8. In this case, the parasitic inductance L_p and the change in parasitic resistance R_{sk} were determined to be:

$$L_P = 8.7 \quad [\text{nH}]$$
$$R_{sk} = 0.52 \times f[\text{MHz}] + 4.7 \times f[\text{MHz}]^2 \quad [\text{m}\Omega] \tag{2.2}$$

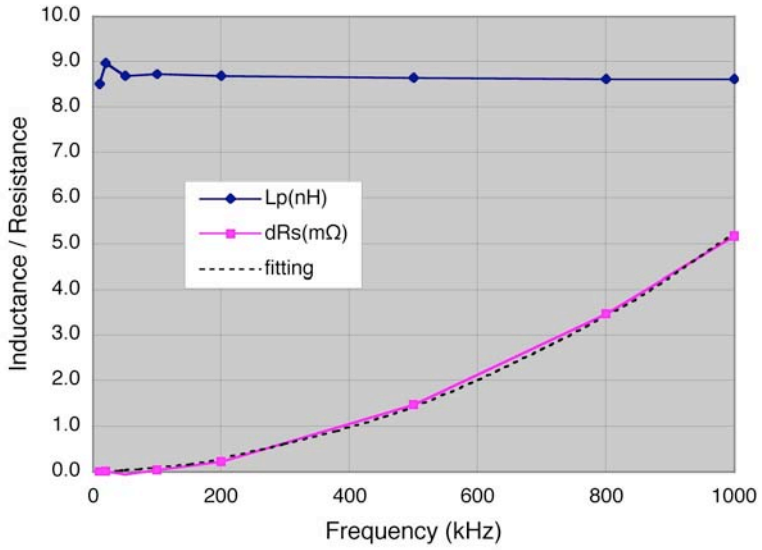

Fig. 2.8. Result of "L_s - R_s" measurement for TVC04.

2.4.2. Stray Capacitance of Heater

To measure the stray capacitance of the heater C_p and dielectric loss component G, the normal JSTC04 element should be replaced with a special "OPEN" element without heater pattern. The stray capacitance and dielectric loss may be measured by "C_p - G" configuration. The circuit connection inside the TVC04, and corresponding circuit model is shown in Fig. 2.9.

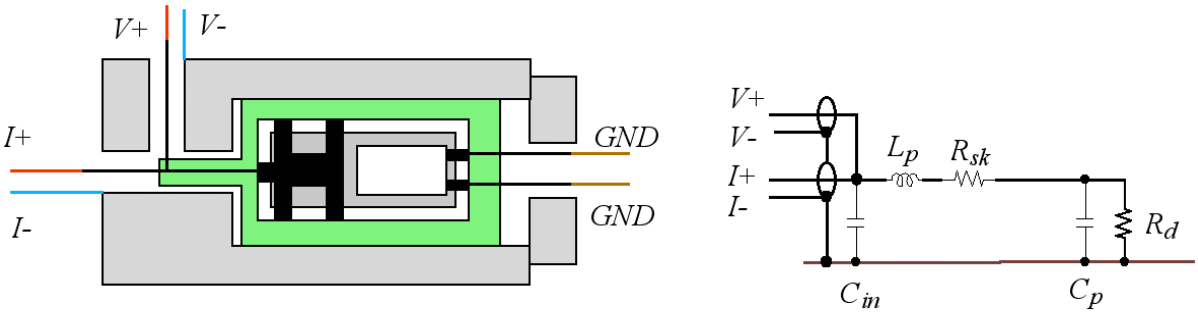

Fig. 2.9. Internal connection and circuit model for "C_p - G" measurement.

The typical results of the measurement are shown in Fig. 2.10. In this case, the stray capacitance of the heater C_p and dielectric loss component G were evaluated to be:

$$C_P = 0.44 \quad [\text{pF}]$$
$$G = 14.5 \times f[\text{MHz}] - 8.7 \times f[\text{MHz}]^2 \quad [\text{nS}] \tag{2.3}$$

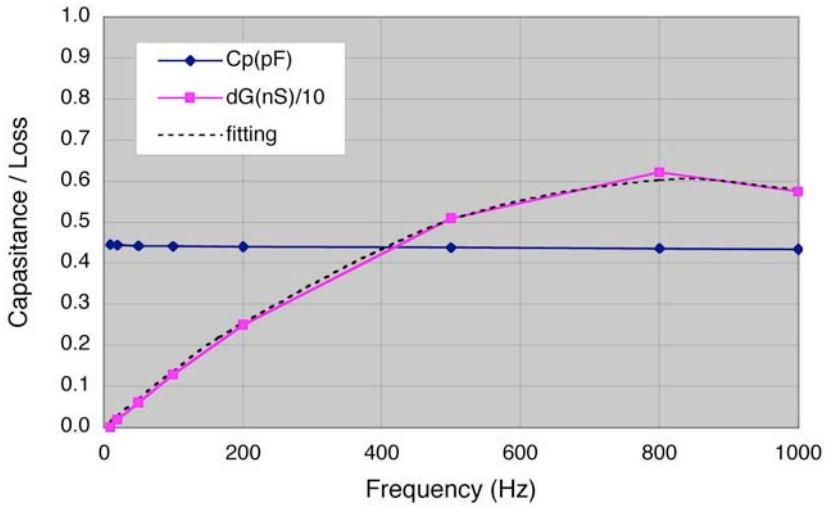

Fig. 2.10. Result of "C_p - G" measurement for TVC04.

2.4.3. Capacitance Between Heater and Thermopile

The parasitic capacitance between the heater and the thermopile $C_{h\text{-}t}$ can be measured with the "OPEN" element at "C_p - G" configuration. The circuit connection inside the TVC04, and corresponding circuit model is shown in Fig. 2.11. The typical value of the parasitic capacitance is

less than 0.1 pF with parallel conductance much smaller than 1 nS. In the case of JSTC04 TC element which has relatively low thermopile resistance (300Ω), the effect to the AC-DC difference at 1 MHz is evaluated using the following equation (2.4) to be smaller than 0.1 ppm at 1MHz.

$$P_C / P_0 = (2\pi f)^2 C^2 r R_t \tag{2.4}$$

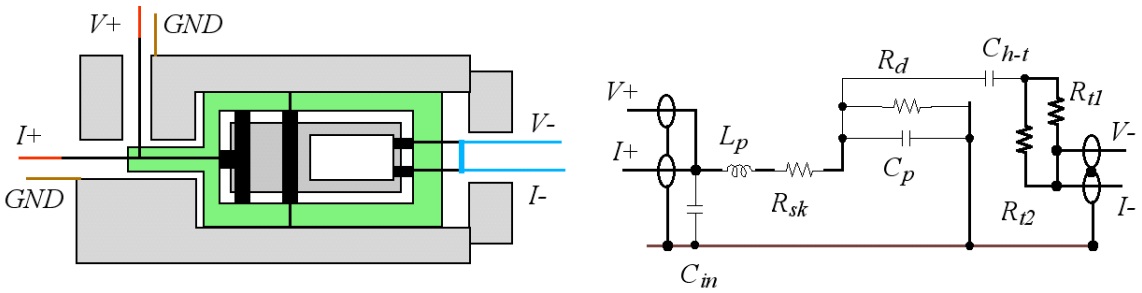

Fig. 2.11. Internal connection and circuit model for measuring input-output coupling.

2.5. Evaluation of Frequency Characteristic

Using the mathematical model and the evaluated values for the parasitic components, the frequency characteristic of the TVC04 can be evaluated using equation (8.1). The asymmetric components of the stray capacitance ΔC, which cannot be measured by an LCR meter, may be assumed as $\Delta C < 2C_p$. The dielectric loss component G may be estimated to be 1/2 of the measured value, because it includes the contribution from the alumina (Si_2O_3) frame that does not contribute to the AC-DC difference. Considering the crudeness of the mathematical model, each component may be attributed with 100% uncertainty with uniform distribution. In the following example, guaranteed maximum values for the parasitic components are used to determine the AC-DC difference for a 500 ohm-input TVC04:

$$\begin{aligned} &L_P < 40 \text{ nH} \\ &R_{sk} < 20 \text{ m}\Omega/\text{MHz} \\ &C_P < 1.0 \text{ pF} \\ &\Delta C_P < 2.0 \text{ pF} \\ &G < 20 \text{ nS}/\text{MHz} \end{aligned} \tag{2.5}$$

Calculated frequency characteristic of the 500 ohm-input TVC04 and its uncertainty are summarized in Table 2.1.

		10 kHz	20 kHz	50 kHz	100 kHz	200 kHz	500 kHz	1000 kHz
LR	Min	0.00	0.00	0.00	0.00	0.01	0.03	0.13
	Max	0.00	0.00	0.00	0.00	0.00	0.00	0.00
LC	Min	0.00	0.00	0.00	0.00	0.00	0.00	0.00
	Max	0.00	-0.01	-0.04	-0.16	-0.63	-3.95	-15.79
CR	Min	0.00	0.00	0.00	0.00	0.00	0.00	0.00
	Max	0.00	0.00	0.00	-0.01	-0.05	-0.31	-1.23
Skin	Min	0.20	0.40	1.00	2.00	4.00	10.00	20.00
	Max	0.00	0.00	0.00	0.00	0.00	0.00	0.00
Loss	Min	0.00	0.00	0.00	0.00	0.00	0.00	0.00
	Max	-0.05	-0.10	-0.25	-0.50	-1.00	-2.50	-5.00
Total	Ave	0.01	0.03	0.07	0.13	0.23	0.33	-0.19
	RSS	0.06	0.12	0.30	0.60	1.20	3.19	7.51

Table 2.1 Contribution of parameters to AC-DC difference (in ppm)

From the results, the frequency dependence in the AC-DC difference of a 500Ω TVC04 and its uncertainties may be formulated as:

$$\gamma_{500\Omega}(1\sigma) \cong (0.0 \pm 7.5) \times 10^{-12} f$$
$$or \qquad . \qquad (2.6)$$
$$\gamma_{500\Omega}[\text{ppm}] \cong (0.0 \pm 7.5) \times f[\text{MHz}]$$

Here, the uncertainty was expressed by a first-order formula that covers the calculated uncertainties at each frequency. The evaluated frequency characteristics of the AC-DC transfer difference for the 500Ω TVC04 are shown in Fig. 2.12. The points specified as "Ave", "+1σ(cal)", and "+1σ(cal)" represents the values given in the table 2.1. The curves specified as "Nom", "+1σ", and "+2σ" represents the values calculated from formula 2.6.

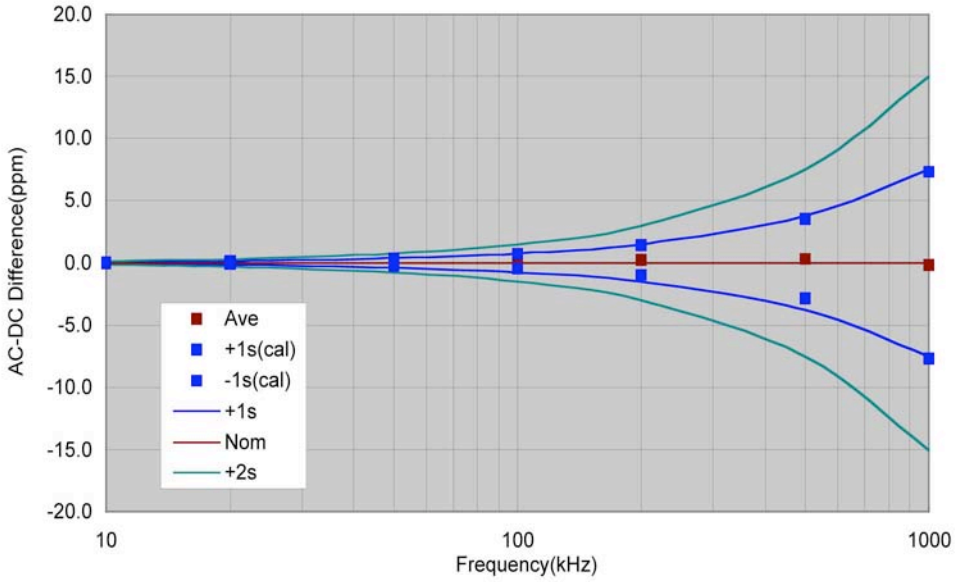

Fig. 2.12 Estimated frequency characteristic of a 500Ω TVC04

2.6. Uncertainty due to Built-in TEE

Another source of uncertainty arises from the use of an N-P plug, to which a test-TVC is connected. As discussed in the previous sections, the N-P plug imitates the half part of the N- RRR TEE connector by which the reference plane is defined. Hence, the difference in the shape and dimension of the N-P plug and the N- RRR TEE connector must be taken as a source of uncertainty in the calibration using the TVC04. In the case of TVC04 with built-in TEE, the uncertainty due to the use of an N-P connector dominates the over-all uncertainties below 100 kHz. The uncertainty may be evaluated experimentally, by adding an extra N-PR connector between TVC04 and test TVC.

Figure 2.13. shows an example of results from ac-ac difference measurement of a TC module (SN05110024) using a TVC04 (SN56001) as a reference standard. From the measurement, the effect of an extra N-PR connector is evaluated to be < 0.8 ppm up to 100 kHz and <2.8 ppm up to 1 MHz. Hence, in the case of a TVC with input resistance of 500Ω, the uncertainty due to the use of built-in TEE can be over-estimated by one-half of the effect, i.e., < 0.4 ppm up to 100 kHz and <1.4 ppm up to 1 MHz.

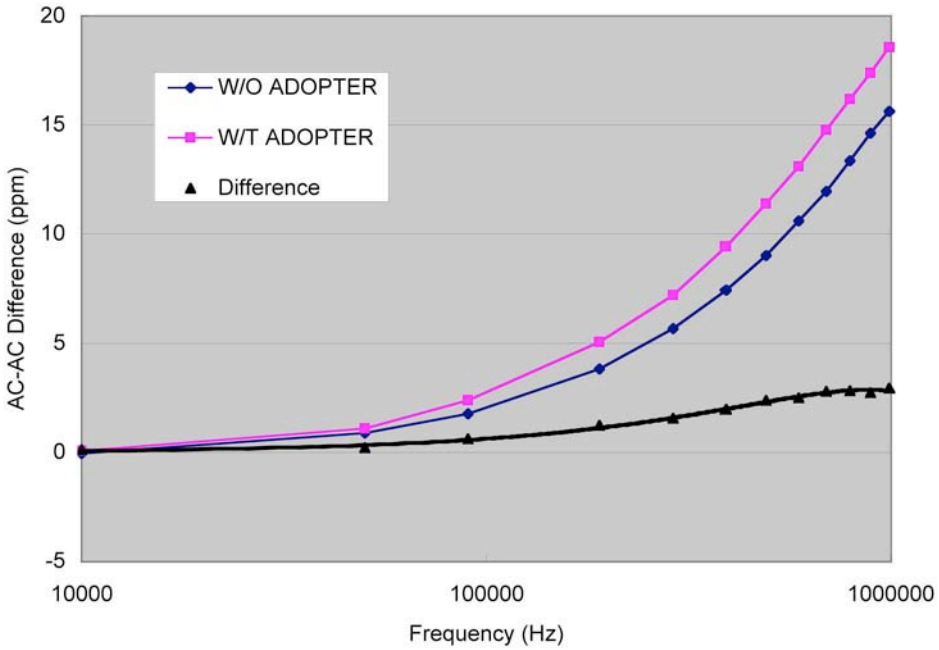

Fig. 2.13. Evaluation of high-frequency characteristic of a TC module.
(with and w/o N-PR connector)

3. Low-Frequency TVC (TVC05)

Low-frequency characteristic of a TVC-input circuit becomes dominant for the AC-DC transfer difference at frequencies lower than 100 Hz. A thermal converter with improved low-frequency performance (TVC05) has been developed at AIST, in collaboration with Nikkohm Co. Ltd. The TVC05 uses a specially designed thermal converter element (JSTC05) optimized for the low-frequency characteristics.

3.1. Type-JSTC05 TC Element

The new Dual-Heater Thermal Converter Element, JSTC05A, is designed to measure the rms voltage of precise alternating waveform at lower frequencies (<10Hz). The structure of JSTC05A, as shown in Fig. 3.1, is almost the same as the single-heater version, JSTC04, except that (1) it has two heater placed side by side (dual-input type), and thickness of the AlN chip is increased from 0.3 mm to 0.63 mm. The heaters have resistances of 100 Ω, with temperature coefficient of 2 ppm to 3 ppm (specified as <10 ppm/K). The time constant is measured to be about 6 second, as expected from the two-fold increase in the thickness of the AlN heater chip. The amplitude of thermally induced ripple from a JSTC05A device in AC-mode at 0.5 Hz was measured to be 2.3% of the total (time-averaged) output voltage. In the case of AC90 mode, the thermally induced ripple was evaluated to be 0.007% of the total voltage, more than two orders of magnitude smaller than in the AC mode.

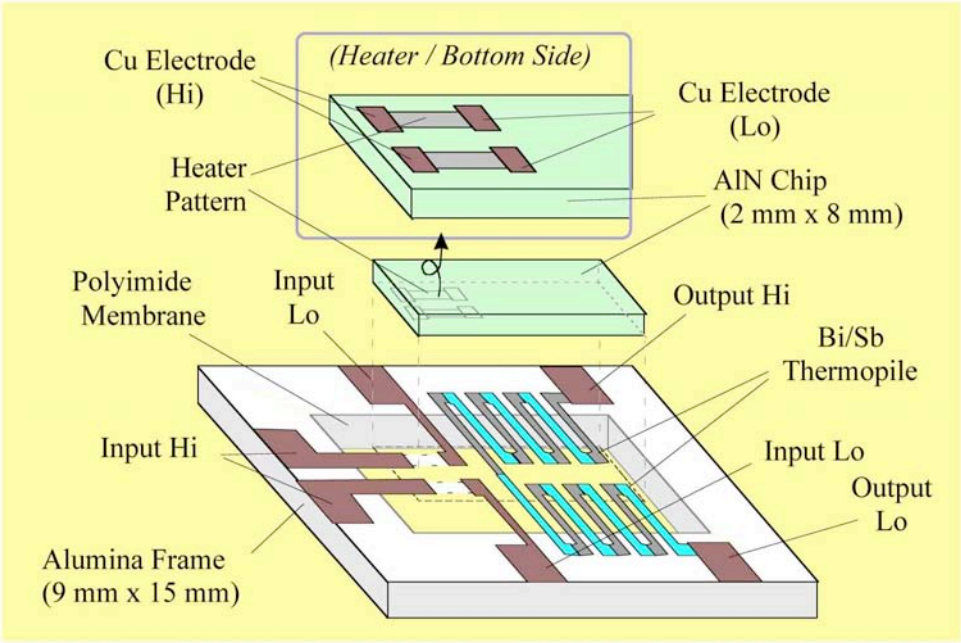

Fig. 3.1. Structure of JSTC05 Thermal Converter Element

3.2. Evaluation of Frequency Characteristics

The low-frequency performance of JSTC05 elements have been evaluated by two methods, using the ET2001 ADS system, i.e., (1) AC-LF measurement and (2) Impedance-matching method. The result of an AC-LF measurement is described in detail in the next subsection 3.2.1, while the Impedance-matching method is described in section 3.2.2. The latter method may be recognized as an alternative method to confirm the validity of the AC-LF measurement.
Another way to evaluate the low-frequency performance is the “90-degrees-addition” method, which utilizes the dual-heater structure of the JSTC05 element. The method and the results of the evaluation is described in section 3.2.3.

3.2.1. AC-LF measurement

The low-frequency performance of JSTC05A has been evaluated by an ACLF measurement. A DSS module was used as a reference standard and the change in the output EMF from the JSTC05A was measured by an AC-AC difference measurement ("ACLF" measurement). In the measurement, the two heaters were connected in series, and a 250 Ω resistor was inserted between the JSTC05A element and the DSS module to improve the impedance matching condition. In this case, the nominal input voltage is 5 V (corresponding to the nominal input current of 10 mA). The output EMF voltage is 16 mA, with dissipation at the heater chip of about 25mW.
The result from the ACLF measurement for a JSTC05A element (#63002) is shown in Fig. 3.2. Test voltage was taken as 3 V, 5 V, and 7V, corresponding to power dissipation of 9 mW, 25 mW, and 48 mW, respectively. Test frequencies were set at 5 Hz up to 200 Hz. The horizontal axis shows the output frequency from the DSS module, and the vertical axis shows the measured AC-AC difference of the JSTC05A element, with reference frequency taken at 77 Hz. The spread of data at 77 Hz (0.3 ppm) represents for the standard deviation of the measurements. Linear offset is added to the result, such that the AC-AC difference between 200 Hz to 77Hz becomes zero for each test voltage. The curve fitting is performed using the following three assumptions:

(1) The rms error in the output voltage from the DSS module is supposed to increase linearly with the output frequency in the frequency range between 5 Hz to 77 Hz.
(2) The effect of the thermal ripple to the AC-AC difference increases linearly with the dissipation power.
(3) The effect of the thermal ripple to the AC-AC difference depends on the test frequency as $(1/f^2)$.

Though more detailed experiment is required to increase the resolution in the measurement, the effect of the thermal ripple seems to be quite small, contributing about 0.1 ppm for nominal power (25 mW) at 10 Hz.

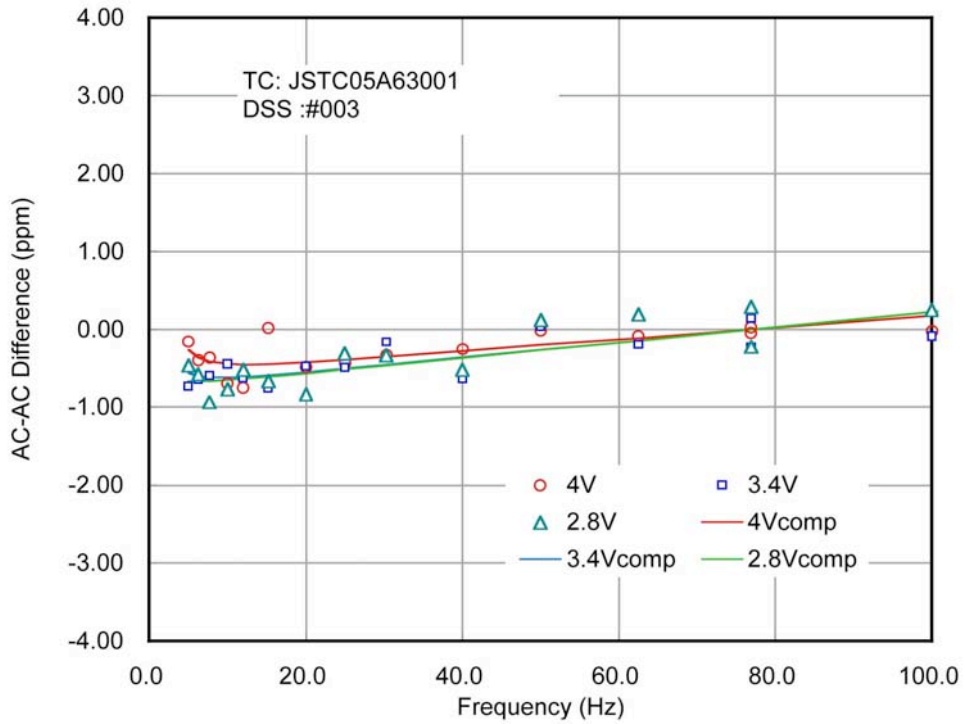

Fig. 3.2. AC-LF Measurement Results for JSTC05A

3.2.2. Impedance-matching method

The impedance-matching method is based on the assumption that the effect of the thermal ripple to the AC-DC difference of a thermal converter increases linearly with the power dissipation at the heater. The circuit diagram for the evaluation of the LF-characteristic of a TVC#1 is shown in Fig. 3.3. The circuit is almost the same as the normal ac-ac difference comparator circuit, except that a "range" resistor R_r of the same resistance as heater resistance R_h is connected in series with the heater of reference TVC#2.

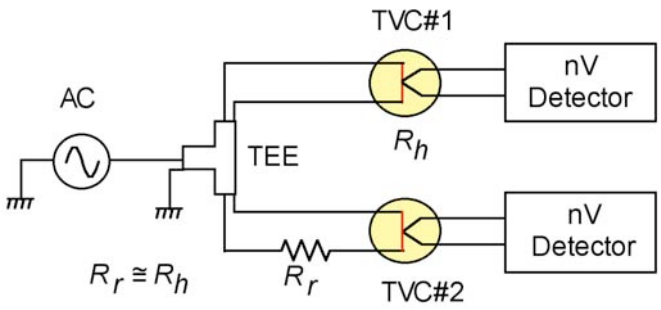

Fig. 3.3. AC-AC Difference Measurement for LF-characteristic of a TVC

In this circuit, the power at the heater is kept constant against the variation of heater resistance, suppressing the effect from the frequency-dependent change in the resistance due to thermal ripple. The amount of joule heating on the reference TVC#2 is also reduced to 25% of the rated power, which itself reduces the amplitude of the thermal ripple by 1/4.

The measurements may be performed at two different configurations, i.e.,

(1) Range resistor on TVC#2 side (Normal Condition).
(2) Range resistor on TVC#1 side (Reverse Condition).

Assuming a reduction factor α_1, α_2 for TVC#1, TVC#2, respectively, The AC-DC difference for the two configuration may be expressed as:

$$\begin{aligned} \delta_{Norm} &= \delta_{TVC\#1} - \alpha_2 \delta_{TVC\#2} \\ \delta_{Rev} &= \alpha_1 \delta_{TVC\#1} - \delta_{TVC\#2} \end{aligned} . \qquad (3.1)$$

From (9.1), the AC-DC difference of the two TVCs (TVC#1, TVC#2) may be evaluated as:

$$\begin{aligned} \delta_{TVC\#1} &\cong (1+\alpha_1\alpha_2)\delta_{Norm} - \alpha_2 \delta_{Rev} \\ \delta_{TVC\#2} &\cong -(1+\alpha_1\alpha_2)\delta_{Rev} + \alpha_1 \delta_{Norm} \end{aligned} . \qquad (3.2)$$

Here the reduction factor α_1, α_2 may be treated as unknown factors smaller than 1/4. Result of a measurement for LF-characteristics using two 2V-input TVC05 (#63001, #63002) is shown in Fig. 3.4. The evaluation was performed at the voltage of 2 V, 3 V and 4 V. The curve fitting is performed using the same assumptions (2) and (3) discussed in the previous sub-section.
From the impedance-matching method, the low-frequency characteristic of the TVC05 (#63001) is estimated to be smaller than 0.1 ppm down to 10Hz.

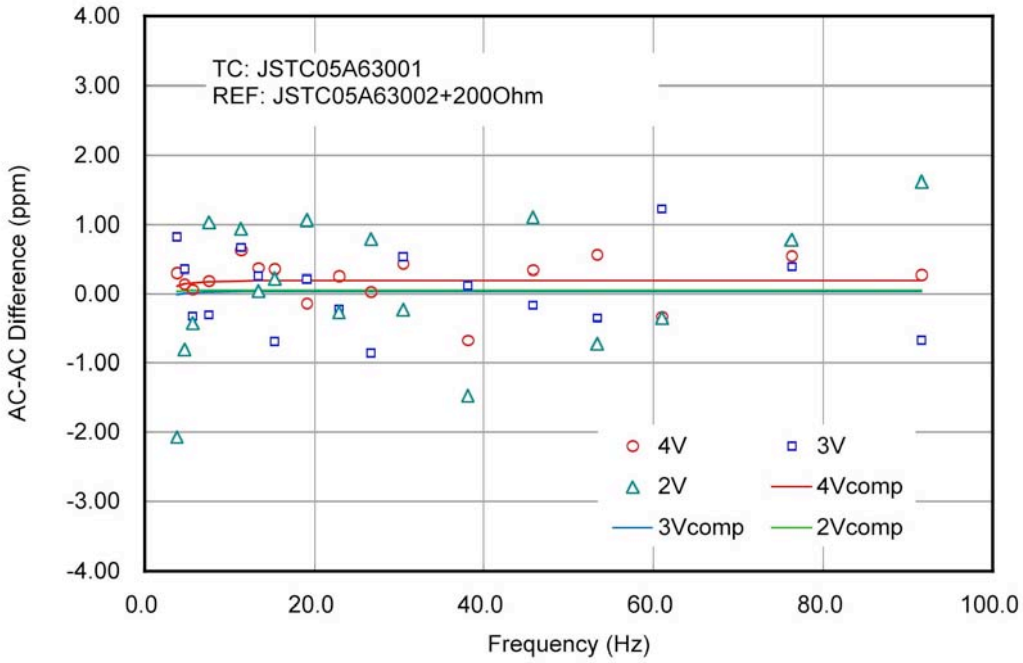

Fig. 3.4. Results from AC-AC difference measurement for TVC05

3.2.3. 90-degrees-addition method

A: Re-Definition of the AC-DC Difference for Dual-Heater TVC

The “90-degree addition method” utilizes the dual-heater configuration of the JSTC05 element, which has a pair of electrically isolated and thermally bound heaters. Applying two sinusoidal waveforms to the two heaters, mutually out of phase by 90 degrees, it is possible to compensate the thermal ripple and suppress the low-frequency characteristics at the lower frequencies. We hereafter specifies the JSTC05 element with two separate inputs as a “DH-TVC”.

In the 90-degree addition method, two measurement conditions are used, i.e., (1) in-phase (AC) mode and (2) 90-degree out-of-phase (AC90) mode. In the in-phase mode (or normal “AC” mode), AC voltages with exactly the same amplitude and the same phase are applied to the two heaters. This condition is physically equivalent to the case when two inputs of the JSTC05 are connected together for the determination of normal (single-input) AC-DC difference. In the case of TVC05B wih single input connector, the two heaters of the JSTC05 element is connected in this way.

In the case of 90-degree out-of-phase mode, AC voltages with relative phase differences of 90 degrees are applied to the two heaters. To distinguish from the normal AC mode, we hereafter call this mode as "AC90" mode. At this mode, the two AC input voltages are mutually out of phase by 90 degrees, and hence the powers dissipated in the heaters are mutually out of phase by 180 degrees. Since the two heaters are thermally bound together, the total power from the two heaters becomes constant and significant reduction in the thermally induced ripple is expected.

The AC-DC difference of a DH-TVC for the two different input conditions can be re-defined in accordance with that for the normal single-heater thermal converters;

$$\delta_{AC-DC} \equiv \left.\frac{V_{AC}-V_{DC}}{V_{DC}}\right|_{E_{AC}=E_{DC}}$$
$$\delta_{AC-AC90} \equiv \left.\frac{V_{AC}-V_{AC90}}{V_{AC90}}\right|_{E_{AC}=E_{AC90}} . \qquad (3.3)$$
$$\delta_{AC90-DC} \equiv \left.\frac{V_{AC90}-V_{DC}}{V_{DC}}\right|_{E_{AC90}=E_{DC}}$$

Since the output voltages E_{AC} and E_{AC90} have pulsating components at lower frequency, it is assumed that time-averages are taken for these quantities. Neglecting second-order contributions due to the difference in the denominators in (1), the normal AC-DC difference of the DH-TVC (δ_{AC-DC}) may be evaluated from the two other quantities ($\delta_{AC-AC90}$ and $\delta_{AC90-DC}$) as;

$$\delta_{AC-DC} \cong \delta_{AC-AC90} + \delta_{AC90-DC} . \qquad (3.4)$$

The relationship between the three quantities in eq. (3.4) is illustrated in Fig. 3.5. The thermal ripple gives significant contribution to AC-DC difference of the DV-TVC below the characteristic frequency ($1/\tau$), where τ represents the thermal time constant of the two heaters. The first term $\delta_{AC-AC90}$ in eq. (3.4) should represent the AC-DC difference of a thermal converter due to the thermal ripple at lower frequencies because, from the thermal viewpoint, the only difference between the AC and the AC90 modes is the presence or absence of thermal fluctuation in the two heaters. The second term $\delta_{AC90-DC}$ includes all the other error-components in AC-DC difference of the DH-TVC. The frequency-independent part of the AC-DC difference due to thermoelectric effects (second-order Thomson or Peltier effect) is also included in $\delta_{AC90-DC}$, because these effects appear only in the DC-input modes.

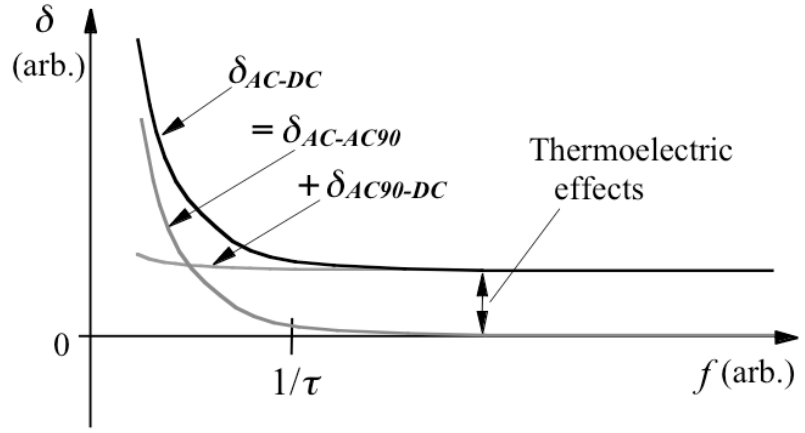

Fig. 3.5. Typical low-frequency characteristic of a DH-TVC.

B: Measurement System

The measurement system uses a PJVS system with a 1-V dual-output PJVS (DO-PJVS) device mounted on a cryo-cooler. The system has the capability to produce the two sinusoidal waveforms with control of the relative phase, required for the 90-degree addition method. The schematic diagram of the measurement setup is shown in Fig. 3.6. The main components of the system are a 1 V dual-output PJVS (DO-PJVS) chip and the dual-heater JSTC05 element (hereafter specified as a "DH-TVC" in this section). Each of the 100 Ω heaters of the DH-TVC requires an input current of 10 mA for the peak input voltage of 1V, while the PJVS device has typical constant-voltage-step width of less than 0.5 mA. Hence high-precision buffer amplifiers, developed by NMIA, were inserted in front of the DH-TVC to enable the connection of the DH-TVC to the PJVS array.

The RMS values of two waveforms generated by the DO-PJVS are applied to the dual inputs of the DH-TVC via the buffer amplifiers, and the EMF output from the DH-TVC is detected by a nV Detector. The DO-PJVS chip is mounted on the cold head of a two-stage G-M cryo-cooler, which can operate the PJVS chip at 10K.

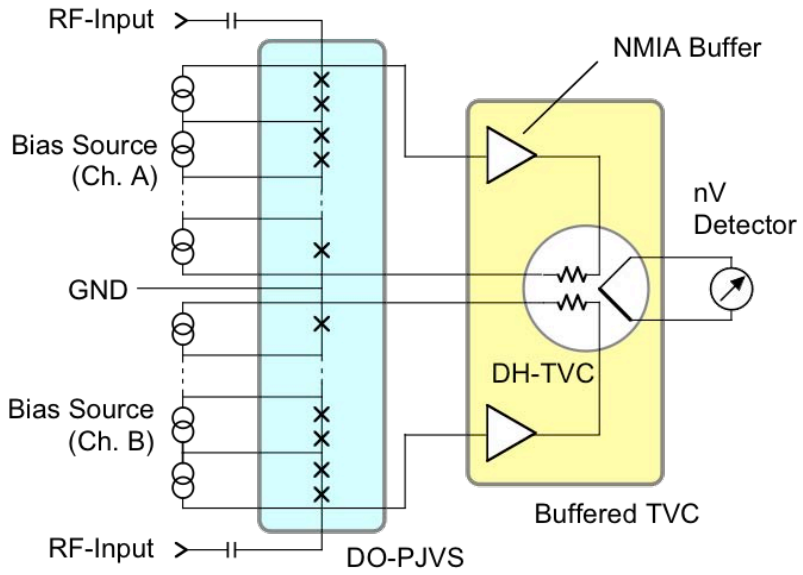

Fig. 3.6. Schematic diagram of the measurement setup.

C: Evaluation of Low-frequency performance of DH-TVC

The low-frequency AC waveforms between 0.1 Hz to 100 Hz were programmed with resolution of bipolar 10 bits (2046 steps peak to peak) in voltage and 7 to 11 bits and with 256 samples per period. The result of the measurements is shown in Fig. 3.7. The error-bars in the figure represent measured standard deviations of the nV-detector reading.

The data points shown by black-circles represent results from the AC-AC90 difference measurement. A large increase in the standard deviation is observed at frequencies below 1 Hz, as expected from the time constant (6 s) of the JSTC05 element, while in the frequency range between 2 Hz to 80 Hz, the AC-AC90 differences are measured to be zero within the resolution of the measurement (0.2 μV/V).

The black-square points represent measured (uncorrected) AC90-DC difference. The standard deviation for the AC90-DC difference measurements does not increase significantly below 1 Hz, unlike the standard deviation of the AC-AC90 difference measurement. This confirms that the combination of dual-heater structure of the DH-TVC and the dual 90-degree out-of-phase outputs of the DO-PJVS are quite effective in reducing the error due to thermal ripple at frequencies below 1 Hz. However, in the frequency range between 2 Hz to 80 Hz, linear frequency dependence of 2.2 (μV/V)/Hz has been observed for the uncorrected AC90-DC difference measurement. If we assume that all the linear frequency dependence comes from the switching transients, then we can subtract this linear dependence (and also the quantization error) and evaluate the "corrected" AC90-DC difference. The corrected AC90-DC differences $\delta_{AC90\text{-}DC}$ are also shown by the white-square points in the Fig. 3.7.

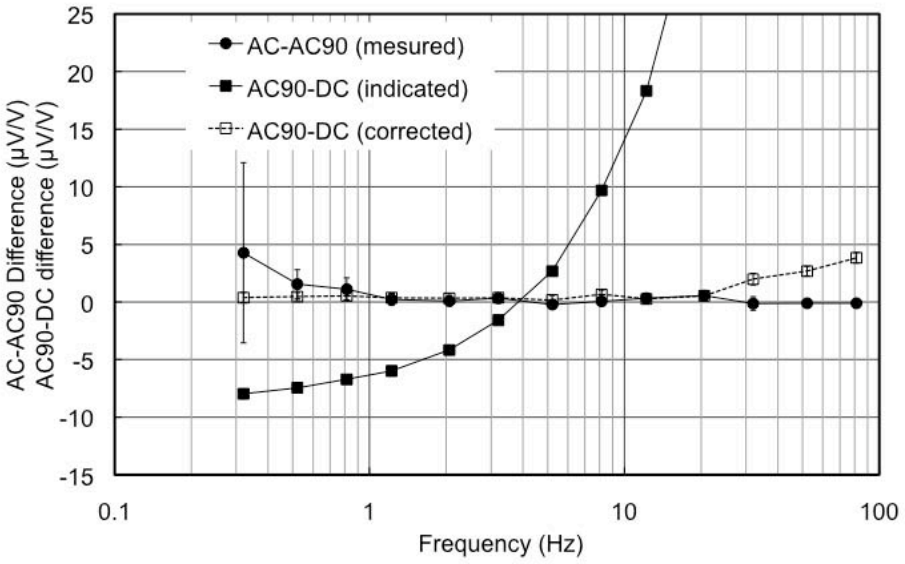

Fig. 3.7. Results from AC-AC90 and AC90-DC difference measurements.

4. General-Purpose TVC (TVC06)

As described in the preceding chapters Ch.2 and Ch.3, both JSTC04 and JSTC05 thermal converter elements were specially designed as a primary reference standard for the high-frequency (>10kHz) and low-frequency (<100 Hz) characteristic in the AC-DC transfer difference, respectively. In order to comply with the strict requirements for the "calculability" of the frequency characteristics, JSTC04 and JSTC05 are fabricated using a complicated "Flip-Chip" bonding process, which tend to reduce both the reliability and production-yield of the elements.

In this chapter, another type of thermal converter element, JSTC06, with improved characteristics for over-all frequency range is described. The JSTC06 elements are implemented in the ET2001 TC modules, and also may be used as general-purpose TVCs for secondary transfer standards.

4.1. Type-JSTC06 TC Element

The structure of the thermal converter element, JSTC06 is shown in Fig. 4.1. The JSTC06 has the same structure for the temperature detection circuit, i.e., a combination of 64 pairs of Bi/Sb thormocouples distributed on both side of the Polyimide membrane. On the other hand, layout of the heater pattern is quite different from that of the previous models. The heater pattern is placed on the opposite side of the AlN chip, and cupper input electrodes are extended via the side-wall of the AlN chip to the back where they are soldered to the cupper input leads on the polyimid membrane. Thickness of the AlN chip is 0.3 mm for standard elements with typical time constant of 2.5 s. The heater-resistance is selectable from 100 Ω to 2k Ω, with temperature coefficient of <25 ppm/K. The JSTC06 element has been developed at Nikkohm Co. Ltd, in collaboration with AIST.

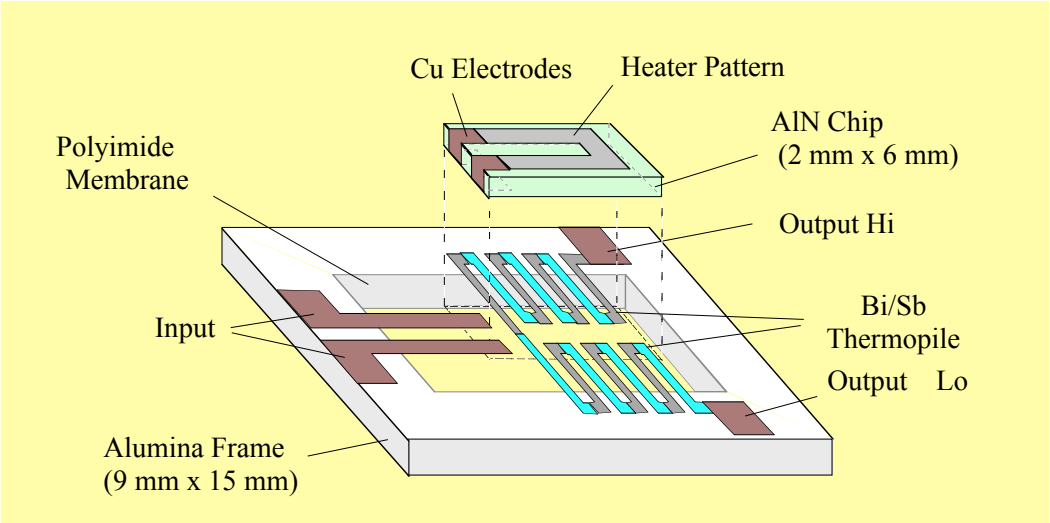

Fig. 4.1. Structure of JSTC06 Thermal Converter Element

4.2. Evaluation of Frequency Characteristics

As described in section 1.3 of the technical reference manual "Guide", the AC-DC transfer difference of the “Reference” TC module is evaluated by the combination of (1) frequency independent DC offset, (2) low-frequency characteristic below 100 Hz, and (3) high-frequency characteristic above 10 kHz. In the following sub-sections, an evaluation of a JSTC06 thermal converter element is described in detail.

4.2.1. DC Characteristics

In the mid-frequency range between 100 Hz and 10kHz, where both the low-frequency effect and the high-frequency effect are negligibly small (<1ppm), the ac-dc difference of a thermal converter is determined by the frequency independent DC offset caused by the Thomson and Peltier effects, as described in the section 1.3.1. To determine the DC offset of a JSTC06 element, FRDC-DC difference measurement has been performed according to the procedure described in section 1.4.1 of this manual and chapter 4 of the technical reference manual "Guide".

The results of the FRDC-DC difference measurements are summarized in Fig. 4.1. The measurement were performed using a JSTC06 element (#02008) at three different voltage levels. As shown in the figure, the FRDC-DC difference was measured to be smaller than 0.5 μV/V in the (reversing) frequency range between 0.1Hz to 10kHz. Hence the DC offset of a JSTC06 element has been assumed to be smaller than 0.5 μV/V.

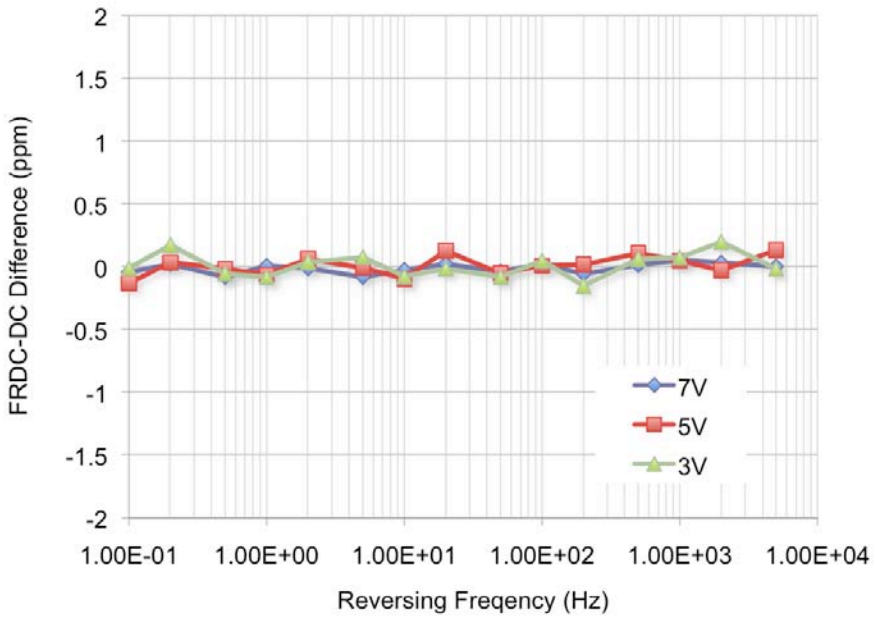

Fig. 4.1. FRDC-DC difference of JSTC06 thermal converter element.

4.2.2. Low Frequency Characteristics

In the frequency range below 100 Hz, the low-frequency effect may become the dominant factor in the AC-DC transfer difference of a JSTC06 thermal converter. As in the case of the JSTC05 elements, the low-frequency characteristic of a have been evaluated by two methods, using the ET2001 ADS system, i.e., (1) AC-LF measurement and (2) Impedance-matching method.

The AC-LF measurement has been performed according to the procedure described in section 1.4.2 of this manual and chapter 5 of the technical reference manual "Guide". The AC-DC difference-comparison measurements for Impedance-matching method were performed according to the procedure described in chapter 6 of the technical reference manual "Guide".

The results of the AC-LF measurement and the Impedance-matching method are summarized in Fig. 4.2. The measurement were performed using a JSTC06 element (#02008) at three different voltage levels. As shown in the figure, the AC-DC difference of the JSTC06 element was evaluated to be smaller than 0.5 μV/V in the low-frequency range between 10Hz to 100Hz.

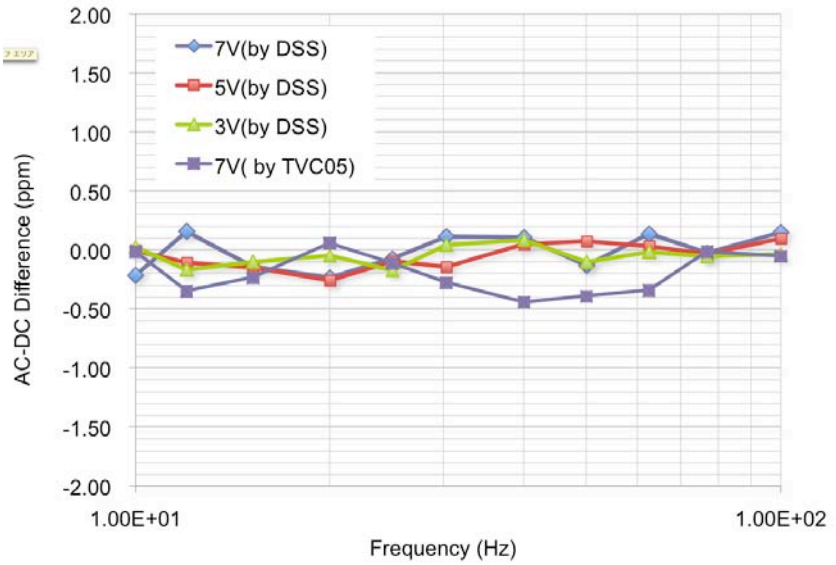

Fig. 4.2. Low-frequency characteristic of a JSTC06 thermal converter element.

4.2.3. High Frequency Characteristics

In the frequency range above 10 kHz, the high-frequency effect due to stray inductance and capacitances becomes the dominant factor in the AC-DC transfer difference of a JSTC06 thermal converter element. The TVC06A has the same chassis as a TVC04 high-frequency thermal converter, except that the element has been replaced by a JSTC06 element instead of the JSTC04. The high-frequency performance of the TVC06A can readily be evaluated using a TVC04 as the reference standard. The high-frequency characteristic of the TVC04 has been evaluated according to the procedure described in chapter 2. The AC-DC difference-comparison measurements between

a 500Ω-input TVC06A (SN#02001) and a 500Ω-input high-frequency TVC (TVC04-500) were performed according to the procedure described in chapter 6 of the technical reference manual "Guide". As both of the TVCs have the virtual TEE configuration, a TC module (SN#ET07) has been used as the intermediate transfer standard.

The results of the AC-DC difference measurements between the TVC06A and the TVC04 are summarized in Fig. 4.3. As shown in the figure, the relative AC-DC difference between the two TVC was measured to be smaller than 1 μV/V in the frequency range between 100 kHz to 1 MHz. Hence a 500Ω-input TVC06A thermal voltage converter may be assumed have the same high-frequency characteristic as that of a 500Ω-input TVC04 within the uncertainty of the measurement.

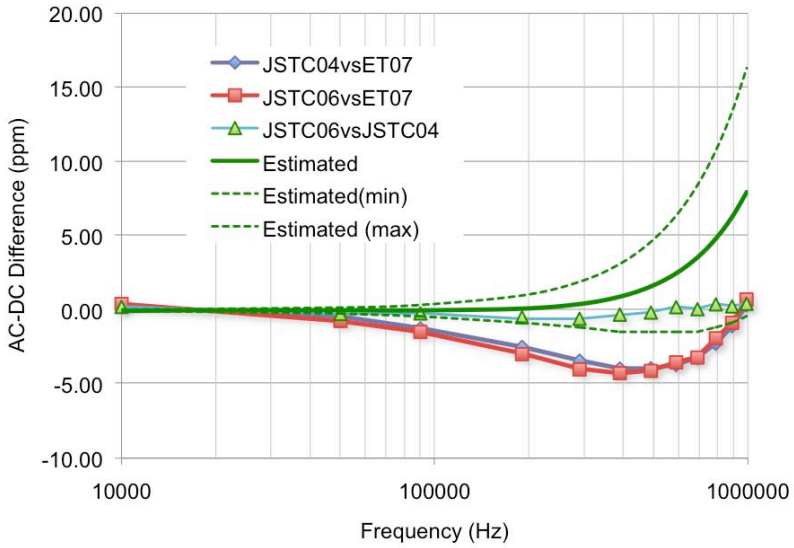

Fig. 4.3. High-frequency characteristic of a JSTC06 thermal converter element.

4.2.4. Over-all Characteristic

To evaluate the chip-to-chip variation in the frequency characteristic, the AC-DC difference-comparison measurement was performed using eight JSTC06 elements from the same lot as SN#02001 and SN#02008. The AC-DC difference of the JSTC06 elements were compared using a TC module (SN#ET07) as the intermediate standard, and measurements were performed according to the procedure described in chapter 6 of the technical reference manual "Guide".

The results are summarized in Fig. 4.3. One of elements (SN#02003) showed a high-frequency characteristic notably different from the other elements and was excluded from the figure. The other seven elements showed a quite similar frequency characteristic as expected, and the relative variation was within 1μV/V between 10 Hz and 100 kHz, and within 10 μV/V up to 1MHz.

The solid red curve shows the estimated frequency characteristics of the TVC06A thermal voltage converter, evaluated by the procedures described in the previous sections 4.2.1 to 4.2.3. The relative variations in the AC-DC difference of each element (from the average of the seven

elements) were plotted with respect to this curve. The dotted red curve (MIN/MAX) represents a measure of criteria for the selection of reliable JSTC06 elements.

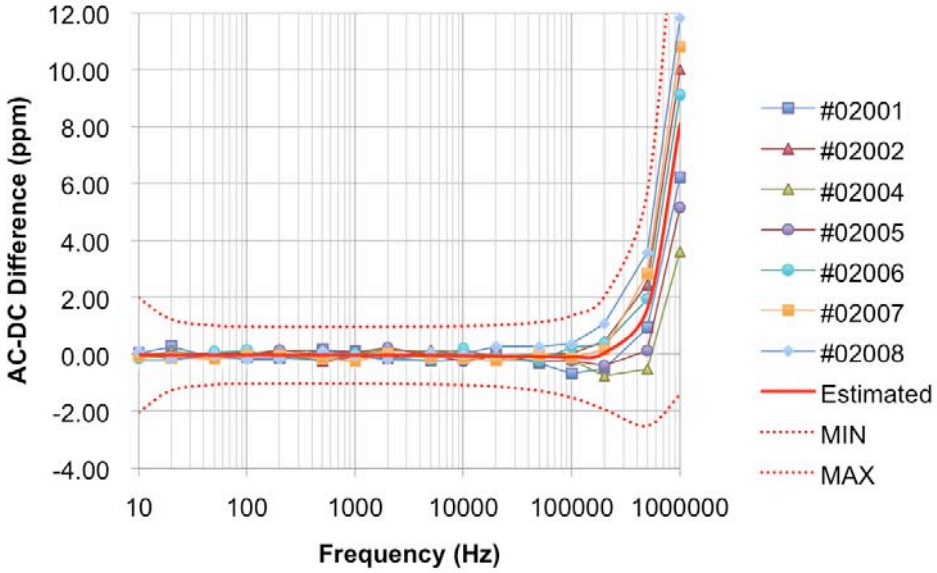

Fig. 4.4. Over-all frequency characteristic of JSTC06 thermal converter elements.

Specifications

4.3. TVC04

Connectors

Input Connector	SMA (Built-in TEE)
Connector to UUT	Type-N
Output Connector	LEMO FBB 3-pin

Thermal Converter

Input Characteristics	
Nominal Resistance Value	50Ω - 2kΩ
Accuracy	± 10%
Parasitic Inductance	<40 nH
Parasitic Capacitance	<1.0 pF
Skin Effect	<20mΩ/MHz
Dielectric Loss	<20nS/MHz
Nominal Input Power	100mW
Absolute Rated Power	0.5W (<1 min)
Output Characteristics	
Output EMF Voltage	60 mV(@100mW)
TC of EMF Voltage	-0.001mV/mW·K (typ.)
Output Resistance	300Ω
Reversal Error	<0.01% (typ.)
Time Constant	2.5 s ± 0.6 s

AC-DC Transfer Difference

10 Hz to 100 kHz	<10 μV/V (typ.)
>100 kHz to 1 MHz	<100 μV/V (typ.)

Miscellaneous

Dimension	2.8 cm x 3.8 cm x 7.4cm
Weight	0.3 kg

4.4. TVC05

Connectors

Input Connector	Type-N
Output Connector	LEMO FBB 3-pin

Thermal Converter

Input Characteristics	
Resistance Value	100Ω x 2
Accuracy	± 10%
Nominal Input Power	50mW
Absolute Rated Power	0.5W (<1 min)
Output Characteristics	
Output EMF Voltage	30 mV(@50mW)
TC of EMF Voltage	-0.001mV/mW·K (typ.)
Output Resistance	<300Ω
Reversal Error	<0.01% (typ.)
Time Constant	6 s ± 1 s
Thermal Ripple	<0.05%@5Hz

AC-DC Transfer Difference

5 Hz to 10 kHz	<10 μV/V (typ.)

Miscellaneous

Dimension	2.8 cm x 3.8 cm x 7.4cm
Weight	0.3 kg

4.5. TVC06

Connectors

Input Connector	SMA (Optional)
Connector to UUT	Type-N
Output Connector	LEMO FBB 3-pin

Thermal Converter

Input Characteristics	
Resistance Value	50Ω - 2kΩ
Accuracy	± 10%
Nominal Input Power	100 mW
Absolute Rated Power	500 mW (<1 min)
Output Characteristics	
Output EMF Voltage	60 mV(@100mW)
TC of EMF Voltage	-0.001mV/mW·K (typ.)
Output Resistance	<300Ω
Reversal Error	<0.001% (typ.)
Time Constant	2.5 s ± 0.6 s

AC-DC Transfer Difference

10 Hz to 100 kHz	<10 μV/V (typ.)

>100 kHz to 1 MHz	<100 µV/V (typ.)

Miscellaneous

Dimension	2.8 cm x 3.8 cm x 7.4cm
Weight	0.3 kg

5. Supplementary Information

5.1. FACs

Q: Should the Shield (chassis) of the thermal converter connected to the Guard (shell of input connector) of the AMP module?
A: Input-Lo and Guard of the AMP module are connected inside. If your thermal converter has internal connection between chassis (Input-Lo) and Output-Lo, you do not have to connect Shield of the thermal converter to the Guard of the AMP module. Please refer to the figures for proper earth and ground connection.

Q: Is it possible to improve detection sensitivity by inserting nanovolt amplifier between the TC and the AMP module?
A: A filter/amplifier specially designed for the thermal converter has been developed at NMIA. Six-fold increase is obtained in the case of SJTC. Contact address <ilya.budovsky@nmia.go.au>.

5.2. Acknowledgements

The TVC04/05/06 thermal voltage converters and JSTC04/05/06 thermal converter elements have been developed through a collaborative research project between Nikkohm Co. and AIST, supported by Shigeru Hidaka, Kaname Kishino, Koji Shimizume of Nikkohm Co. The ET2001 AC-DC transfer standard (ADS) has been developed through a collaborative research project between SunJEM Co. and AIST. Detailed designing of the ADS was performed by Minoru Usuda and Shinichi Koyano of SunJEM Co., Japan, and Shinzo Honda of Yatoro-Electronics Co., Japan. Contribution and Supports from Hiroyuki Fujiki of AIST and Kunihiko Takahashi of JEMIC are gratefully acknowledged.

5.3. Contact Address

[Purchase information]

Nikkohm Co., Ltd
FAX: +81-176-53-2106
Email: service@nikkohm.com
Or
Key Techno Co., Ltd.
Fax: +81-3-3251-3166
Email: keytechno@pop14.odn.ne.jp

[Technical questions or comments]

Nikkohm Co., Ltd
FAX: +81-176-53-2106
Email: service@nikkohm.com
http://www.nikkohm.com
or
Hitoshi SASAKI
Nanoelectronics Research Institute, AIST
Email: hitoshi-sasaki@aist.go.jp